Published in final edited form as:
J Am Chem Soc. 2009 October 7; 131(39): 13952–13962. doi:10.1021/ja905080e.

Structure-Reactivity Effects on Primary Deuterium Isotope Effects on Protonation of Ring-Substituted α-Methoxystyrenes

Wing-Yin Tsang and **John P. Richard***
Contribution from the Dept. of Chemistry, University of Buffalo, SUNY, Buffalo, NY 14260-3000.

Abstract

Primary product isotope effects (PIEs) on L^+- and carboxylic acid-catalyzed protonation of ring-substituted α-methoxystyrenes (**X-1**) to form oxocarbenium ions **X-2**$^+$ in 50/50 (v/v) HOH/DOD were calculated from the yields of the α-CH_3 and α-CH_2D labeled ketone products, determined by ^{1}H NMR. A plot of PIE against reaction driving force shows a maximum PIE of 8.7 for protonation of **4-MeO-1** by $Cl_2CHCOOH$ (ΔG^o = 1.0 kcal/mol). The PIE decreases to 8.1 for protonation of **4-MeO-1** by L_3O^+ (ΔG^o = −2.8 kcal/mol) and to 5.1 for protonation of **3,5-di-NO_2-1** by $MeOCH_2COOH$ (ΔG^o = 13.1 kcal/mol). The PIE maximum is around ΔG^o = 0. Arrhenius-type plots of PIEs on protonation of **4-MeO-1** and **3,5-di-NO_2-1** by L_3O^+ and on protonation of **X-1** by $MeOCH_2COOH$ in 50/50 (v/v) HOH/DOD give similar slopes and intercepts. These were used to calculate values of $[(E_a)_H - (E_a)_D]$ = −1.2 kcal/mol and (A_H/A_D) = 1.0 for the difference in activation energy for reactions of A–H and A–D and for the limiting PIE at infinite temperature, respectively. These parameters are consistent with reaction of the hydron over an energy barrier. There is no evidence for quantum mechanical tunneling of the hydron through the barrier. These PIEs suggest that the transferred hydron at the transition state lies roughly equidistant between the acid donor and base acceptor, and contrast with the recently published Brønsted parameters [Richard, J. P.; Williams, K. B. *J. Am. Chem. Soc.* **2007**, *129*, 6952–6961], which are consistent with a product like transition state. An explanation for these seemingly contradictory results is discussed.

Introduction

Brønsted acid-base-catalyzed proton transfer at carbon (eq 1) is an apparently simple, but profoundly important reaction in chemical and biological processes.[1] The results of investigations of the effect of changing substituent –X at the base catalyst and –Y at the carbon acid on rate constants for proton transfer provide considerable insight into the bonding changes that occur on proceeding from reactants to transition state. [2–6] This experimental work defines the relative free energies for the formation of a large number of transition states, and has allowed investigators to draw inferences about transition state structure, without the direct observation of these species. By comparison, computational studies have the potential to provide a more detailed description of the reaction coordinate profile and transition state structure for proton transfer at carbon.[7–12] However, there is no general agreement about which computational methods are adequate for their intended purpose, particularly for the modeling of acid-base-catalyzed proton transfer at carbon in water. This provides a simple rationale for continued experimental studies on proton transfer at carbon - these are needed to provide the large body

jrichard@buffalo.edu.

Supporting Information Available: Table S1 – S4 of observed product isotope effects, $(PIE)_{obs}$, for reactions of **X-1** in 50/50 (v/v) HOH/DOD that contains different concentrations of lyonium ion or Brønsted acid catalysts, and at different reaction temperatures. This material is available free of charge via the Internet at http://pubs.acs.org.

of data required to demonstrate that modern computational results are able to reproduce experimental reaction rate and equilibrium constants.

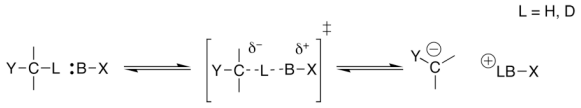

(1)

There have been relatively few studies in recent years on kinetic isotope effects on proton transfer at carbon, despite the clear need for experimental data to evaluate the contribution of the pathway for quantum mechanical tunneling to the observed rate constants for these proton transfer reactions.13–18 We recently reported a fast, convenient and general method to determine primary product isotope effects (PIEs) on proton transfer reactions in hydroxylic solvents.[19] This method was used to determine PIEs on protonation of ring-substituted α-methoxystyrenes **X-1** by lyonium ion (Scheme 1) over a broad range of temperature and thermodynamic driving force (Scheme 1).[19] We now report the full details of our experiments to determine PIEs, and extensive new data for protonation of **X-1** by carboxylic acids. Our work was initiated with the following goals in mind.

We wanted to increase the number of experimental determinations of isotope effects on protonation of structurally homologous carbon bases, that may be directly compared with the isotope effects determined in computational studies. We have compared these experimentally determined isotope effects with isotope effects calculated using a novel approach based on Kleinert's variational perturbation theory within the framework of Feynman path integrals.[20–22]

Primary kinetic isotope effects on Brønsted acid-catalyzed reactions in water are normally estimated from the ratio of second-order rate constants for reactions in HOH and DOD.[23] We wanted to show that these primary isotope effects might be determined more easily and accurately from the ratio of H- and D-labeled products of protonation of **X-1** in the common solvent of 50/50 HOH/DOD.

We recently reported the effect of changing reaction driving force on the Brønsted structure-reactivity coefficients α and β, determined for variations in the acidity of the carboxylic acid proton donor, and in the basicity of the vinyl ether proton acceptor **X-1**, respectively.[24] We wanted to compare these changes in Brønsted parameters with the corresponding changes in the kinetic isotope effect for the protonation of **X-1**, in order to more fully define the changes in transition state structure that occur with changing reaction driving force.

Two explanations have been offered to explain the changes in primary isotope effects on hydron transfer at carbon that have been observed to occur with changing reaction driving force:[23, 25] (a) These changes may be due to changes in the structure of the transition state for the hydron transfer reaction;[26,27] or, (b) They may be due to changes in the relative importance of the reaction by hydron transfer over a reaction barrier, which shows a primary KIE of *ca* 7, compared to the reaction of the hydron by quantum-mechanical tunneling through the barrier, which shows a much larger KIE.[25] We have therefore examined the temperature dependence of the PIE on protonation of **X-1** by lyonium ion and by a carboxylic acid, in order to evaluate the importance of tunneling.

Experimental Section

The procedures for the preparation of 3,5-dinitroacetophenone and ring-substituted α-methoxystyrenes, and the sources for the other reagents used in this work were given in an earlier publication.[24] Solvents were used without further purification unless otherwise indicated. Water was first distilled and then further purified with a Milli-Q water apparatus. Deuterium labeled water (99.9% D), DCl (35% w/w, 99.9%D) and KOD (40% wt, >98%D) were purchased from Cambridge Isotope Laboratories.

^{1}H NMR Analyses

^{1}H-NMR spectra at 500 MHz were recorded on a Varian UNITY INOVA 500 MHz spectrometer as described in earlier work.[28,29] The following relaxation times T_1 were determined in $CDCl_3$ for the α-CH_2D protons of the monodeuteriated ring substituted acetophenones: 3,5-dinitroacetophenone, 3 s; 4-methoxyacetophenone, 3 s; 4-nitroacetophenone, 3 s compounds; and, acetophenone, 4s. ^{1}H-NMR spectra of the products of hydrolysis of **X-1** in 50/50 (v/v) HOH/DOD (a mixture of α-CH_3 and α-CH_2D labeled ketone **X-3**) were recorded in $CDCl_3$ (30 – 60 transients) with a pulse angle of 90°, an acquisition time of 7–10s, and a relaxation delay of $7T_1$. All spectra were referenced to $CHCl_3$ at 7.27ppm, and base lines were drift-corrected before integration of the signals due to the α-CH_3 and α-CH_2D groups.

Preparation of Solutions

The concentrations of solutions of strong acids and bases were standardized by titration using phenolphthalein as an indicator. A stock solution of 50/50 (v/v) HOH/DOD, obtained by mixing equal volumes of HOH and DOD, was used to prepare solutions of KCl. A 4.5 M solution of LO^- and a 1.0 M solution of LCl in 50/50 (v/v) HOH/DOD were prepared, respectively, by mixing equal volumes of 4.5 M KOH and 4.5 M KOD or of 1.0 M HCl and 1.0 M DCl.

Solutions of CH_3COOL in 50/50 (v/v) HOH/DOD were prepared by adding equal molar amounts of CH_3COOH and CH_3COOD to 50/50 (v/v) HOH/DOD. Other solutions of carboxylic acids in 50/50 (v/v) HOH/DOD were prepared by dissolving the acid RCO_2H in 50/50 (v/v) HOH/DOD and then adding a small amount of D_2O to balance the acidic hydrogen of RCO_2H. These solutions were adjusted to the appropriate $[RCO_2L]/[RCO_2^-]$ ratio by adding measured amounts of KOL in 50/50 (v/v) HOH/DOD.

Product Studies

The hydrolysis of **X-1** was initiated by making a 1/100 dilution of the reactant in acetonitrile into acidic solutions of 50/50 (v/v) HOH/DOD (v/v) (I = 1.0 KCl) to give the following final substrate concentrations: **4-MeO-1**, 0.3 mM in 25 mL of 50/50 (v/v) HOH/DOD; **H-1**, 0.8 mM in 10 mL of 50/50 (v/v) HOH/DOD; **4-NO_2-1**, 0.09 mM in 50 mL of 50/50 (v/v) HOH/DOD; and, 3,5–**di-NO_2-1**, 0.06 mM in 50 mL of 50/50 (v/v) HOH/DOD.

The halftimes for hydrolysis of **X-1** in dilute solutions of LCl were estimated using second-order rate constants determined for hydrolysis in HOH and DOD,[24,30] and assuming a linear dependence of the observed rate constant on the deuterium composition of solvent. Acidic solutions of 50/50 (v/v) HOH/DOD were vortexed during the addition of the reactive substrate **4-MeO-1** in order to ensure rapid mixing. In cases where the halftime for the specific acid- and buffer-catalyzed solvolysis in 50/50 HOH/DOD (v/v) was > 1 minute, a 1.0 mL aliquot was transferred to a cuvette immediately after initiation, and the reaction was monitored by UV-spectroscopy.[24] The lyonium-ion and buffer-catalyzed reactions of **4-MeO-1** were quenched (see below) after a 1 – 5 minute reaction time, which was at least 10 halftimes for

the hydrolysis reaction of **4-MeO-1**. The hydrolysis reactions of other **X-1** were monitored by UV spectroscopy, and allowed to proceed to at least 50% conversion to ketone product **X-3**.

These reactions were quenched by extraction of the organic material into 1 – 2 mL of $CDCl_3$ at the following reaction times: **H-1**, 7 – 10 reaction halftimes; **4-NO_2-1**, 1 – 7 reaction halftimes, depending upon the buffer catalyst; **3, 5-di-NO_2-1**, 1 – 5 reaction halftimes, depending upon the buffer catalyst. The organic layer was separated from the aqueous layer using a disposable pipette and then dried by filtration through a short column of $MgSO_4$ directly into an NMR tube. The samples were stored at −15 °C for one or two days, until the analysis for deuterium enrichment of the α-carbonyl methyl group using ^{1}H NMR. It has been shown that the α–hydrogen of a simple methyl ketone are stable to exchange for at least one month under these conditions.[31] The reactions at elevated temperatures (> 25 °C) were rapidly cooled to room temperature in an ice bath prior extraction of products into $CDCl_3$.

The ratio of the yields of products of solvolysis of **X-1** in 50/50 (v/v) HOH/DOD (I = 1.0 KCl) labeled with an α-CH_3 and an α-CH_2D group was determined using eq 2, where A_{CH3} is the area of the singlet due to the -CH_3 group and A_{CH2D} is the area for the downfield shifted triplet (J_{HD} = 2 Hz) due to the -CH_2D group: **MeO-3**, δ = 2.553 (CH_3), 2.536 ppm, (CH_2D); **H-3**, 2.614 (CH_3), 2.598 ppm (CH_2D); **4-NO_2-3**, 2.681 (CH_3), 2.665 ppm (CH_2D); **3,5-di-NO_2-3**, 2.777 (CH_3), 2.761 ppm (CH_2D).

$$(\mathrm{PIE})_{\mathrm{obsd}}=\frac{[\mathrm{P_H}]}{[\mathrm{P_D}]}=\frac{A_{\mathrm{CH_3}}}{1.5A_{\mathrm{CH_2D}}} \tag{2}$$

Kinetic Studies

The hydrolysis of **X-1** in 50/50 (v/v) HOH/DOD at 25 °C (I = 1.0 KCl) was monitored by UV spectroscopy.[24] The observed first-order reaction rate constants and second-order rate constants for Brønsted acid catalysis were determined as described in earlier work.[24]

Deuterium Exchange Reactions of X-3—The exchange of the α-CH_3 hydrogen of **X-3** for deuterium in 50/50 (v/v) HOH/DOD (I = 1.0 KCl) was monitored at 25 °C. The exchange reactions were initiated by making a 100-fold dilution of **X-3** in acetonitrile into 50/50 (v/v) HOH/DOD (I = 1.0 KCl) to give the following final substrate concentrations and reaction volumes: **4-NO_2-3**, 0.09 mM in 250 mL solvent; and, **3,5-diNO_2-3**, 0.08 mM in 250 mL solvent. At timed intervals, 50 mL of the reaction mixture was withdrawn, the organic material was extracted into 1 – 2 mL of $CDCl_3$ and the organic layer was dried as described above.

$$\frac{A_{\mathrm{CH2D}}}{A_{\mathrm{CH3}}+1.5A_{\mathrm{CH2D}}}=(k_{\mathrm{obs}})\mathrm{t} \tag{3}$$

$$k_{\mathrm{A}}=k_{\mathrm{obs}}/[\mathrm{A}^-] \tag{4}$$

The first-order rate constant, k_{obs} (s^{-1}), for the deuterium exchange reaction of the α-CH_3 group of **X-3** to form the α-CH_2D group was determined as the slope of a plot of reaction progress against time over the first 5 – 10% of the reaction (eq 3), where A_{CH3} is the area of the singlet due to the CH_3 group of the reactant and A_{CH2D} is the area for the downfield shifted triplet due to the CH_2D group of the product. The second-order rate constant for the carboxylate anion-catalyzed exchange reaction was determined according to eq 4, where [A^-] is the concentration of the buffer base for the particular experiment.

Products of solvolysis of 4-nitroacetophenone dimethyl ketal

This ketal was prepared as a 0.25 M solution in acetonitrile that contained 0.5 mM of the internal standard fluorene. Solvolysis was initiated by making a 100-fold dilution of the ketal into water buffered with potassium phosphate at pH 6.7. The ketone (of **4-NO_2-3**) and alkene (**4-NO_2-1**) reaction products were separated by HPLC and the product ratio was determined from the ratio of the HPLC peak areas A_{alk}/A_{ket}, and using $\varepsilon_{Ket}/\varepsilon_{alk} = 0.17$ for the ratio of the extinction coefficients of **4-NO_2-3** and **4-NO_2-1**. The product ratio [alkene]/[ketone] decreased slowly with time, due to acid-catalyzed conversion of **4-NO_2-1** to **4-NO_2-3**. The initial ratio of product yields was determined by making a small (< 20%) linear extrapolation to zero time of a plot of A_{alk}/A_{ket} against time.

RESULTS

A second-order rate constant of $k_L = 500\ M^{-1}\ s^{-1}$ for hydrolysis of **4-MeO-1** in 50/50 (v/v) HOH/DOD (I = 1.0, KCl) at 25 °C was estimated as the average of the values of $k_H = 870\ M^{-1}\ s^{-1}$ [24] and $k_D = 170\ M^{-1}\ s^{-1}$ [30] for the reactions in HOH and DOD, respectively. The hydrolysis reaction of **4-MeO-1** was examined at lyonium ion concentrations ranging from 3 mM to 11 mM, where the estimated halftimes for hydrolysis is between 0.5 and 0.12 s. These acidic solutions of 50/50 (v/v) HOH/DOD were vigorously vortexed during addition of substrate **4-MeO-1** in order to ensure rapid mixing of the reactant.

Figure 1 shows the partial 500 MHz NMR spectrum, using two different scales for the *y*-axis, of **H-3** that forms as the product of the lyonium-ion-catalyzed reaction of **H-1** in 50/50 (v/v) HOH/DOD (I = 1.0, KCl) at 25 °C. These spectra are similar to those reported in earlier determinations of deuterium enrichment of carbon acids using ^{1}H NMR.[28,29,31–39] The major peak is the singlet for the α-CH_3 group of **H-3** formed by reaction with L_2OH^+, and the smaller peaks are the 0.016 ppm upfield-shifted triplet for the α-CH_2D group of **H-3** formed by reaction with L_2OD^+. The observed product isotope effect $(PIE)_{obs}$ for protonation of **H-1** is equal to the ratio of the integrated areas of the peaks for the –CH_3 and –CH_2D groups (eq 2). A small 0.3%/D isotope effect has been reported for partitioning of H- and D-labeled alkanes between methanol/water mixtures and the solid support of a C_{18} reverse phase HPLC column, with –H showing a slight preference for the hydrophobic environment.[40] A small isotope effect on partitioning of the –H and –D labeled **X-3** between $CDCl_3$ and water would have been too small to be detected by these experiments, and so this partitioning isotope effect is assumed to be negligible.

The values of $(PIE)_{obs}$ for the L_3O^+-catalyzed reactions of **X-1** in 50/50 (v/v) HOH/DOD (I = 1.0, KCl) at 25 °C are reported in Table S1 of the Supporting Information. Figure 2 shows the values of $(PIE)_{obs}$ determined for hydrolysis of **4-MeO-1** and **3,5-di-NO_2-1** in the presence of different $[L_3O^+]$. In all cases, the variation in the values $(PIE)_{obs}$ for the reaction of **X-1** (X = 4-OMe, 4-H, 4-NO_2, 3,5-di-NO_2) at different $[L_3O^+]$ is less than ± 2%. The product isotope effects on protonation of **X-1** by lyonium ion [$(PIE)_L$, eq 5 and Scheme 2], calculated as the average of the $(PIE)_{obs}$ determined for reactions at five different $[L_3O^+]$, are reported in Table 1.

The interpretation of these data would become problematic, if the first-order rate constants for addition of solvent to **X-2$^+$** and for deprotonation to form **X-1** were similar. This is because the apparent PIE for hydrolysis of **X-1** in 50/50 (v/v) HOH/DOD would depend upon the true PIE on protonation of **X-1** and a second isotope effect on the partitioning of –CH_3 and –CH_2D labeled **X-2$^+$** between addition of water and deprotonation to reform **X-1**.[41] We have therefore examined the effect of increasing $[AcO^-]$ on the yield of the products of solvolysis of 4-nitroacetophenone dimethyl ketal in water that contains 10 mM phosphate buffer at pH 6.7 and 25 °C. The solvolysis gives very low yields of alkene **4-NO_2-1** (> 0.1 %). This shows

that > 99.9% of the **4-NO_2-2**$^+$ intermediate of hydrolysis of **4-NO_2-1** would partition forward to product under these conditions. The rate constant ratio k_{AcO}/k_s = 0.0011 M was determined as the slope of a plot (not shown) of product yields ([**4-NO_2-1**]/[**4-NO_2-3**]) against [AcO^-].

Carboxylic acids are very effective catalysts of the protonation of **X-1**, which is the ratedetermining step for hydrolysis of **X-1** to form **X-3** (Scheme 1). The values of $(PIE)_{obs}$ for the reactions of **X-1** in the presence of carboxylic acid catalysts in 50/50 (v/v) HOH/DOD (*I* = 1.0, KCl) at 25 °C, determined by ^{1}H NMR analysis, are reported in Table S2 of the Supporting Information.

Figure 3A shows that there is only a small change in the value of $(PIE)_{obs}$ for protonation of **4-MeO-1** as $[LA]_T$ is increased from 0.20 to 0.80 M. This is because the PIEs on the lyonium ion- and on the buffer-catalyzed reactions are similar. The buffer-catalyzed reaction is the major pathway even when concentrations of buffer are low ($[P_H]_{LA} >> [P_H]_L$ and $[P_D]_{LA} >> [P_D]_L$, eq 7]. The product isotope effects on protonation of **4-MeO-1** by carboxylic acids [$(PIE)_{LA}$, eq 6)] in 50/50 (v/v) HOH/DOD, determined as the average of the values of $(PIE)_{obs}$ observed at the three highest concentrations of the carboxylic acid catalyst, are reported in Table 1.

$$(PIE)_L = \frac{[P_H]_L}{[P_D]_L} \quad (5)$$

$$(PIE)_{LA} = \frac{[P_H]_{LA}}{[P_D]_{LA}} \quad (6)$$

$$(PIE)_{obs} = \frac{[P_H]_L + [P_H]_{LA}}{[P_D]_L + [P_D]_{LA}} \quad (7)$$

Figure 3B shows that the value of $(PIE)_{obs}$ for protonation of **H-1** does not change significantly as $[LA]_T$ is increased from 0.16 to 0.64 M. This reflects the strong buffer catalysis of protonation of **H-1**.[24] PIEs on protonation of **H-1** by carboxylic acids [$(PIE)_{LA}$] in 50/50 (v/v) HOH/DOD, determined as the average of the values of $(PIE)_{obs}$ observed at the three highest concentrations of the carboxylic acid catalyst, are reported in Table 1.

The general base-catalyzed deuterium exchange reaction of **X-3** is normally much slower than the hydrolysis of **X-1**. For example $k_A = 7.9 \times 10^{-7}$ M^{-1} s^{-1} [42] for deprotonation of acetophenone (**H-3**) by acetate anion in water, and the rate constant for the deuterium exchange reaction of **H-3** in 50/50 (v/v) HOH/DOD will be 4–5 fold smaller, because of the discrimination isotope effect against protonation of the acetophenone enolate by LOD in the mixed solvent. By comparison, rate constants $k_{HA} \geq 6.6 \times 10^{-5}$ M^{-1} s^{-1} were reported for protonation of **X-1** in water.[24]

It would have been difficult to obtain a reliable value of $(PIE)_{LA}$ for the relatively slow protonation of **3,5-di-NO_2-1** by CH_3CO_2L, because the *apparent* yield of the D-labeled product increased by *ca* 20% during CH_3CO_2L-catalyzed hydrolysis in 50/50 (v/v) HOH/DOD. We attribute the additional D-labeled *product* at later reaction times to a competing acetate anion-catalyzed deuterium exchange reaction of **3,5-di-NO_2-3**. We have therefore compared directly the rate constants for carboxylate anion-catalyzed deuterium exchange reactions of **4-**

NO_2-3 and **3,5-di-NO_2-3** and for carboxylic acid-catalyzed protonation of **4-NO_2-1** and **3,5-di-NO_2-1** in 50/50 (v/v) HOH/DOD (Table 3). This comparison shows that the ketone product of hydrolysis of **3,5-di-NO_2-1** catalyzed by Brønsted acids *more reactive* than CH_3CO_2L, or of hydrolysis of aryl vinyl ethers *more reactive* than **3,5-di-NO_2-1** is stable to exchange over several halftimes of the vinyl ether hydrolysis reaction. For example, $k_{HA} = 2.8 \times 10^{-4}$ M^{-1} s^{-1} for methoxyacetic acid-catalyzed hydrolysis of **3,5-NO_2-1** in 50/50 (v/v) HOH/DOD at 25 °C is 230-fold larger than $k_A \approx 1.2 \times 10^{-6}$ M^{-1} s^{-1} for the methoxyacetate anion-catalyzed deuterium exchange reaction of **3,5-NO_2-3**.

The ratio of –H and –D labeled ketone products for the methoxyacetic acid-catalyzed hydrolysis of **3,5-NO_2-1** (Table S2) were determined after *ca* one reaction halftime, where there can be no significant methoxyacetate acetate anion-catalyzed deuterium exchange reaction of the ketone product. For example, only a 24 minute reaction time was used for hydrolysis of **3,5-NO_2-1** in 50/50 (v/v) HOH/DOD that contained 0.80 M MeOAcOH buffer ($[HA]/[A^-] = 7/3$) at 25 °C (Table S2). A control experiment with 0.80 M MeOAcOH buffer, at an even higher pL ([HA] = 0.08 M, $[A^-] = 0.72$ M), showed that only 12% of the α-CH_3 groups of **3,5-NO_2-3** underwent deuterium exchange after 2400 minutes. A second control showed that identical values $(PIE)_{obs} = 5.5 \pm 0.1$ were determined for protonation of **3,5-NO_2-1** in 0.80 M methoxyacetic acid buffer ($[HA]/[A^-] = 9$) at several times up 1230 minutes, which is 35 halftimes for the hydrolysis reaction (Table S2).

Figure 4 shows the change in $(PIE)_{obs}$ with increasing concentrations of carboxylic acid buffers for the hydrolysis of **4-NO_2-1** (Figure 4A) and **3,5-di-NO_2-1** (Figure 4B) **1** in 50/50 (v/v) HOH/DOD at 25 °C. The second-order rate constants for the lyonium ion- and buffer-catalyzed reactions in the same solvent are reported in Table 2. The data in Table 2 show that for many of these hydrolysis reactions both the lyonium ion- and buffer-catalyzed pathways contribute to the observed reaction rate constants. Now, the value of $(PIE)_{obs}$ decreases with increasing concentrations of buffer, because $(PIE)_{LA} < (PIE)_L$. Table 1 reports the values of $(PIE)_{LA}$ for protonation of **4-NO_2-1** and **3,5-di-NO_2-1** by carboxylic acids that were determined from the nonlinear least-squares fit of the data from Figure 4A and 4B to eq 8, using the values of k_L and k_{LA} (M^{-1} s^{-1}) from Table 2, $(PIE)_L$ from Table 1, and treating $(PIE)_{LA}$ as a variable parameter. The four terms in eq 8 correspond to the normalized velocities for product formation by the four pathways in eq 7 ($[P_H]_L$, $[P_D]_L$, $[P_H]_{LA}$ and $[P_D]_{LA}$).

$$(PIE)_{obs} = \frac{k_L[L^+]\left(\frac{(PIE)_L}{1+(PIE)_L}\right) + k_{LA}[LA]\left(\frac{(PIE)_{LA}}{1+(PIE)_{LA}}\right)}{k_L[L^+]\left(\frac{1}{1+(PIE)_L}\right) + k_{LA}[LA]\left(\frac{1}{1+(PIE)_{LA}}\right)} \quad (8)$$

The product isotope effect on protonation of **4-MeO-1** by lyonium ion at 278 K, calculated as the average of the $(PIE)_{obs}$ (Table S3) determined for reactions at four different $[L_3O^+]$, is reported in Table 3. The reactions of **4-MeO-1** at 319 K were examined at four different low concentrations of acetic acid buffer (40% free base) between 3 – 12 mM. The increase in k_{obs} for hydrolysis of **4-MeO-1**, from 0.0104 to 0.0165 s^{-1} as the buffer concentration is increased from 3 – 12 mM (Table S3), corresponds to an increase from 20% to 50% in the contribution of the buffer-catalyzed pathway of the total reaction with the remaining reaction being due to catalysis by L_3O^+. The value of $(PIE)_{obs} = (PIE)_L = 6.9 \pm 0.1$ was found to be independent of buffer concentration (Table S3).We conclude that the PIEs on the lyonium ion and buffer-catalyzed reaction are essentially identical, as was also observed for the acetic acid-catalyzed reaction at 298 K (Table 3).

The reactions of **4-MeO-1** at 343 K were examined in the presence of four different concentrations of acetic acid buffer (70% free base) between 3 – 12 mM. The increase in

k_{obs} for hydrolysis, from 0.011 to 0.021 s^{-1} as the concentration of the buffer is increased from 3 – 12 mM (Table S3), corresponds to an increase from 30% to 65% in the contribution of the buffer-catalyzed pathway of the total reaction. The value of $(PIE)_{obs} = (PIE)_L = 5.87 \pm 0.03$ determined for these reactions are independent of buffer concentration (Table S3), so that the PIEs on the lyonium ion and buffer-catalyzed reaction are identical within experimental error. A control experiment at 343 K with the ketone **4-MeO-3** in 50/50 (v/v) HOH/DOD that contains 12 mM acetate buffer (70% free base) showed that there was no detectable deuterium exchange over a period of 10 minutes, which is 60-haltimes for the hydrolysis of **4-MeO-1** under these conditions.

Product isotope effects on the reactions of **3,5-di-NO_2-1** at 313, 328, 343 and 359 K at different $[L_3O^+]$ are summarized in Table S3. In all cases $(PIE)_{obs}$ is independent of $[L_3O^+]$. The value of $(PIE)_L$ for lyonium ion protonation of **3,5-di-NO_2-1** at each temperature was calculated as the average of the values $(PIE)_{obs}$ determined at four different $[L_3O^+]$ (Table 3).

The yields of the H- and D-labeled products formed after *ca* 10-halftimes of methoxyacetic acid-catalyzed hydrolysis of **H-1** in 50/50 (v/v) HOH/DOD (I = 1.0, KCl) and at several different temperatures were determined by ^{1}H NMR. The values of $(PIE)_{obs}$ for experiments at 277 K ($[MeOCH_2CO_2^-]/[MeOCH_2CO_2H] = 9$) are summarized in Table S4. The experiments at 321 and 343 K were carried out at $[A^-]/[AH] = 99$, and using a constant concentration of 10 mM acetic acid buffer to maintain pH. There is more than a doubling in k_{obs} for hydrolysis of **H-1** at 321 and 343 K as ($[MeOCH_2CO_2^-] + [MeOCH_2CO_2H]$) is increased from 0.10 – 0.45 M, but no change in $(PIE)_{obs}$ (±3 %) (Table S4). Therefore, there is no detectable difference in the PIE for reactions catalyzed by the different acids present in solution. The values of $(PIE)_{AL}$ reported in Table 3 for methoxyacetic acid-catalyzed hydrolysis of **H-1** were calculated as the average of the values $(PIE)_{obs}$ determined at four different ($[MeOCH_2CO_2^-] + [MeOCH_2CO_2H]$) (Table S4). Short reaction times of < 5 minutes were used for the reaction at 343 K in order to guarantee that there was no base-catalyzed exchange of deuterium from solvent into product **H-3**.

Discussion

There is good evidence that protonation of **X-1** to form **X-2$^+$** is *effectively* irreversible, and the rate-determining step for the hydrolysis of **X-1** to form **X-3**.[23,46–48] If so, then the PIEs determined for the hydrolysis of **X-1** are equal to the primary isotope effects on protonation of these carbon bases. We have examined the partitioning of **X-2$^+$** (Scheme 3) in order to quantify the *irreversibility* of protonation of these vinyl ethers. The value of $k_{AcO}/k_s = 0.0011$ M reported here for partitioning of **4-NO_2-2$^+$** between deprotonation and addition of water (Scheme 3), shows that **4-NO_2-2$^+$** formed as an intermediate of protonation of **4-NO_2-1** by acetic acid rarely returns to **4-NO_2-1**. A value of $k_{AcO}/k_s = 0.0034$ M has been reported for the partitioning of **H-2$^+$**,[24] and $k_{AcO}/k_s = 0.0057$ M for partitioning of **4-MeO-2$^+$** may be calculated from $k_s = 7 \times 10^6$ s^{-1} and $k_{AcO} = 4.0 \times 10^4$ M^{-1} s^{-1}.[24,48,49] The partitioning of **3,5-NO_2-3$^+$** was not examined, because changes from electron-donating to electron-withdrawing ring substituents at **X-2$^+$** cause k_{AcO}/k_s to decrease (*vida infra*), so that $k_{AcO}/k_s < 0.0011$ M for partitioning of this oxocarbenium ion.

These data show that hydrolysis of **4-MeO-1** has the greatest tendency towards reversibility. Return to alkene becomes more favorable with decreasing acidity of the acid catalyst, because of a corresponding increase in the basicity of its conjugate base. Even in the most unfavorable case for catalysis by acetic acid, **4-MeO-2$^+$** returns to reactant only ≈ 3/1000 times that it is generated by protonation of **4-MeO-1** by 1.0 M acetic acid ($[AH]/A^- = 1.0$).

Isotope effects on hydron transfer from solvent or from Brønsted acids that undergo fast hydron exchange with solvent can be determined either as the ratio of rate constants (k_H/k_D) for reactions in HOH and DOD (a KIE),[23] or as the ratio of the hydrogen and deuterium labeled products (eq 2) of reaction in 50/50 (v/v) HOH/DOD (a PIE). The KIE on hydron transfer is generally simpler to measure than the PIE, because the kinetic determination does not require analytical methods to distinguish between H- and D- labeled products. On the other hand, the uncertainty in second-order rate constants k_L is generally ± 5% so that the uncertainty in the KIE determined from a rate constant ratio will be *ca* ± 10%. By comparison, the values of $(PIE)_{obs}$ for protonation of **X-1** determined by ^{1}H NMR analysis are generally reproducible to better than ±2%. The precision of the measurements of the ratio of ^{1}H NMR peak areas is potentially better than ± 2%.[50]

The interpretation of the PIEs determined in this work is simpler than interpretation of earlier KIEs on the protonation of vinyl ethers.[23] The primary deuterium isotope effect, and the secondary solvent deuterium isotope effect both contribute to the magnitude of the KIE determined from the rate constant ratio k_H/k_D for reactions in HOH and DOD.[51] By comparison, the PIE is obtained from the yields of –H and –D labeled products from a reaction in 50/50 (v/v) HOH/DOD, and provides a direct measure of the relative reactivity of these two isotopes in a common solvent.[51]

Catalysis by Lyonium Ion and by Brønsted Acids

The value of $(PIE)_L$ or $(PIE)_{AL}$ (Table 1) for these Brønsted acid-catalyzed reactions is equal to the equilibrium constant for exchange of –H and –D at the transition state for hydron transfer in 50/50 (v/v) HOH/DOD ($1/\phi_{TS}$, where ϕ_{TS} is referred to as the fractionation factor) when $x = 0.50$ for the mole fraction of –D in solvent (eq 9).[52,53] The value of $1/\phi_{TS}$ defines the relative stability of the –H and –D labeled transition states compared to a common ground state of 50/50 (v/v) HOH/DOD. The kinetic isotope effect (k_{AH}/k_{AD}) is defined by Eyring theory as the ratio of equilibrium constants for conversion of the H- and D-labeled Brønsted acids to the corresponding transition states for protonation of **X-1** ($K^{\pm}_{AH}/K^{\pm}_{AD}$, Scheme 4). Eq 10, derived for Scheme 4, shows that the KIE and the PIE are simply related by the equilibrium constant $1/\phi_{AL}$ for exchange of –H and –D at the Brønsted acid (eq 11).[52,53]

$$1/\Phi_{TS} = (PIE)_{AL} = \frac{[SH]^{\pm}(x)}{[SD]^{\pm}(1-x)} \tag{9}$$

$$(KIE)_{AL} = \left(\frac{k_{AH}}{k_{AD}}\right) = \left(\frac{K^{\pm}_{AH}}{K^{\pm}_{AD}}\right) = \frac{\Phi_{AL}}{\Phi_{TS}} = \Phi_{AL}(PIE)_{AL} \tag{10}$$

$$1/\Phi_{AL} = \frac{[AH](x)}{[AD](1-x)} \tag{11}$$

Eqs 9 and 10 show that the PIE is directly related to the partitioning of –H and –D between a common ground state of 50/50 (v/v) HOH/DOD and the transition state for hydron transfer, while the KIE measures the relative barriers to moving from -H and -D labeled Brønsted acids to the transition state. The PIE and the KIE are different when the H/D enrichment of the Brønsted acid catalyst is different from the enrichment of solvent ($\phi_{AL} \neq 1.0$, eq 10), as is the case for L_3O^+-catalyzed reactions ($\phi_{AL} = \phi_{L3O} = 0.69$).43,[44] The value of $(KIE)_L$ for the

L_3O^+-catalyzed reaction provides a measure of the change in the fractionation of –H compared with –D between 50/50 (v/v) HOH/DOD at the reactant compared with the transition state. Correction of the values of $(PIE)_L$ in Table 1 for the preferential fractionation of -H from solvent to lyonium ion catalyst ($\phi_{L3O} = 0.69$) gives the values of $(KIE)_L$ reported in this Table. Table 1 also reports values of $(KIE)_{AL}$ for protonation of **X-1** by acetic acid, calculated from the $(PIE)_{AL}$ and $\phi_{AL} = 0.90$ (eq 10).[45]

We will focus in this paper on the product isotope effects $(PIE)_L$ and $(PIE)_{AL}$, because their changes with changing reaction driving force are due *solely* to changes in transition state structure, as measured by $1/\phi_{TS}$. By comparison, the KIE depends upon ϕ_{AL} for the reactant and ϕ_{TS} for the transition state, so that changes in reactant ϕ_{AL} with changing driving force will affect the KIE (eq 10). Note, for example, that the difference between the KIEs for the lyonium-ion-catalyzed and the acetic acid-catalyzed reactions (Table 1) are partly due to the difference in the fractionation factors for the two Brønsted acid catalysts.

Secondary Solvent Deuterium Isotope Effects

The rate constant ratio $k_H/k_D = 4.0$ for L^+-catalyzed hydrolysis of **H-1** in pure HOH ($k_H = 85$ M^{-1} s^{-1})[24] and in pure DOD ($k_H = 21$ M^{-1} s^{-1})[30] at 25 °C and $I = 1.0$ (KCl) reflects the total changes in bonding at the transferred -L and the two "stationary" -L of L_3O^+. The primary $(KIE)_L = 5.7$ for protonation of **H-1** in 50/50 HOH/DOD (Table 1) shows that the *zero-point energy* of the transferred -L is largely lost at this transition state (see below); and, when combined with $k_H/k_D = 4.0$ gives a value of 4.0/5.7 = 0.70 for the secondary solvent deuterium isotope effect (SDIE) on this reaction. This solvent isotope effect represents the contributions of bonding changes at the nonreacting hydrons to the ratio $k_H/k_D = 4.0$. The isotope effect is due to a *tightening* of the O-L bonds at these "non-reacting" hydrons on proceeding from L_2O-L^+, where these O-L bonds are weakened by strong hydrogen bonds to solvent, to a transition state that has advanced towards product L-O-L that forms weaker hydrogen bonds to solvent.[51,54] A rough estimate of the fractional progress α of the reactants towards the transition state can be obtained using eq 12, where $(\phi_{L3O})^2 = 0.48$ [43,44] is the maximum SDIE for a product-like transition state (α = 1.0).[51,54] Substitution of SDIE = 0.70 and $(\phi_{L3O+})^2 = 0.48$ into eq 12 gives α = 0.48. This corresponds to a transition state that is roughly at the midpoint between reactant L_2O-L^+ and product L-O-L with respect to changes in the hydrogen-bonding interactions between the solvent and the nonreacting hydrons of L_2O-L^+

$$\alpha = \frac{\log (\mathrm{SDIE})}{\log (\phi_{L3O+})^2} \qquad (12)$$

Temperature dependence of PIEs

Figure 5A shows Arrhenius-type plots of the PIEs for protonation of **4-MeO-1** and **3,5-di-NO_2-1** in 50/50 (v/v) HOH/DOD. The following slopes and intercepts were determined by linear least squares analysis of the data from Figure 5A: **4-MeO-1**; slope of $-[(E_a)_H - (E_a)_D]/R = 630 \pm 30$ K and intercept $\ln(A_H/A_D) = -0.048 \pm 0.11$; **3,5-di-$NO_2$-1**, slope of 590 ± 19 K and intercept −0.001 ± 0.06 (the quoted errors are standard deviations). These give values of $[(E_a)_H - (E_a)_D] = -1.25$ and −1.17 kcal/mol and $(A_H/A_D) = 1.00$ and 0.95, respectively, for protonation of 4-**MeO-1** and **3,5-di-NO_2-1** by L_2OH^+ and L_2OD^+. Figure 5B shows the linear Arrhenius-type plot of $(PIE)_{AL}$ for protonation of **H-1** by methoxyacetic acid in 50/50 (v/v) HOH/DOD, constructed using data from Table 3. The slope of this plot is $-[(E_a)_H - (E_a)_D]/R = 595$ K ± 30, and the intercept is $\ln (A_H/A_D) = 0.02 \pm 0.10$. These give values of $[(E_a)_H - (E_a)_D] = -1.18$ kcal/mol and $(A_H/A_D) = 1.02$ for protonation of **4-H-1** by methoxyacetic acid.

The average value of $[(E_a)_H - (E_a)_D] = -1.2$ kcal/mol determined from these Arrhenius-type plots is remarkably close to the value of -1.21 kcal/mol for the difference in zero-point energy for ground state hydrons at LO-H and LO-D (Δzpe), calculated from "first principles" using eq 13,[55] where $\nu_H = 3400$ is the IR stretching frequency for the LO-H bond [56] and $\nu_H/\nu_D = 1/1.35$ is the ratio of stretching frequencies for LO-H and LO-D bonds.[55] This provides good evidence that most or all of the zero-point-energy of the solvent LO-L bond is lost at the transition state for protonation of **X-1** by Brønsted acids.

$$\Delta zpe = -1/2hc\,(\nu_H - \nu_D) = -1/2hc(1 - 1/1.35)\,\nu_H \quad (13)$$

PIE and reaction driving force

Figure 3B, Figure 4A and 4B for the reactions of **H-1**, **4-NO_2-1**, and **3,5-di-NO_2-1**, respectively, provide the following insight into the relationship between the magnitude of the PIE and the reaction driving force.

The value of $(PIE)_L$ for catalysis by lyonium ion (*y*-intercept, Figure 3 and Figure 4) is generally equal to or larger than value of $(PIE)_{obs} = (PIE)_{AL}$ for reactions in the presence of large concentrations of carboxylic acid catalysis; and, the values of $(PIE)_{AL}$ decrease with increasing pK_a of the carboxylic acid catalyst. This shows that these PIEs generally decrease as the proton transfer reaction becomes more unfavorable thermodynamically. On the other hand, the *difference* between $(PIE)_L$ for catalysis by L_3O^+ and $(PIE)_{AL}$ for catalysis by methoxyacetic acid increases as the reactivity of the vinyl ether substrate is decreased by electron-withdrawing ring substituents. For example, $(PIE)_L = 8.2$ and $(PIE)_{AL} = 7.6$, respectively, for protonation of **H-1** by L_3O^+ and methoxyacetic acid, while $(PIE)_L = 7.3$ and $(PIE)_{AL} = 5.1$ for protonation of **3,5-di-NO_2-1** by the same two acids.

These trends are also shown in the logarithmic plot (Figure 6) of isotope effects against the change in the reaction standard Gibbs free energy ($\Delta G° = -RTln K_{eq}$, Scheme 5),[24] where the range of values of $\Delta G°$ on the *x*-axis is 16 kcal/mol.[24] The solid symbols in Figure 6 are PIEs, and the open symbols are KIEs that were calculated from the PIE using eq 10. Note that similar PIEs for reactions in 50/50 HOH/DOD are observed for L^+- and carboxylic acid-catalyzed reactions of similar driving force. This confirms that the difference in the KIEs determined for protonation of **X-1** by L^+- and carboxylic acids in pure HOH and DOD is due essentially entirely to difference in secondary solvent deuterium isotope effects on proton transfer (see above).

Figure 6 shows that the maximum PIE of *ca* 8.7 is observed for the nearly thermoneutral ($\Delta G° = 1.0$ kcal/mol) protonation of **4-MeO-1** by $Cl_2CHCOOH$. There is a falloff in this isotope effect to 8.1 for thermodynamically favorable protonation of **4-MeO-1** by L_3O^+, and a falloff to 8.0 for protonation of **H-1** by $CNCH_2COOH$ as the reaction becomes thermodynamically favorable ($\Delta G° = 5.1$ kcal/mol). The result is a broad region that runs from $\Delta G° = -2.8$ kcal/mol to $\Delta G° = 5.1$ kcal/mol where the change in PIE with changing reaction driving force is relatively small (0.7 units). There is then a steeper change in PIE with changing driving force, as shown by the decrease in the $(PIE)_L = 8.0$ for protonation of **H-1** by cyanoacetic acid to $(PIE)_{AL} = 5.1$ for protonation of **3,5-di-NO_2-1** by methoxyacetic acid (Figure 4B) as $\Delta G°$ increases from 5.1 to 13.1 kcal/mol.

An isotope effect maximum at $\Delta G° \approx 0$ kcal/mol similar to that shown in Figure 6 has been reported in earlier studies of the KIEs on Brønsted base-catalyzed deprotonation of –H and –D labeled α-carbonyl carbon acids.[57] The rate constants ratio k_H/k_D for lyonium ion-catalyzed hydrolysis of substituted vinyl ethers in HOH and DOD also show a maximum at intermediate reactivity.[23] However, the values of $\Delta G°$ for these reactions *were not determined.* The scatter

in the earlier experimental data is much greater than for Figure 6 and this resulted in very poorly defined isotope effect maxima. For example, nearly the same value of $k_H/k_D = 2.6$ is observed for specific acid-catalyzed hydrolysis of 4-methylene-1,3-dioxane ($k_H = 6.5\ M^{-1}\ s^{-1}$) and methyl *trans*-propenyl ether ($k_H = 0.072\ M^{-1}\ s^{-1}$), despite the *ca* 100-fold difference in the second-order rate constants for these reactions.[23] The extensive scatter in these earlier plots of KIE against reaction driving force represents partly or entirely the very large structural diversity of reactants in comparison with structurally homologous substrates **X-1**.

The complete equations for kinetic isotope effects published by Bigeleisen and Mayer[58] can be used to rationalize both small and large kinetic isotope effects, and changes in these isotope effects.[59] Two explanations have been proposed to explain the changes in primary kinetic isotope effect responsible for bell-shaped plots of primary isotope effects against reaction driving force, and the centering of the isotope effect maximum on $\Delta G^o = 0$.[25]

(1) The change in the primary isotope effect may reflect a change in the fraction of the zero-point energy of the reactant A-H bond that is maintained in the symmetrical stretching vibration at the transition state (Scheme 6), as described by Melander and Westheimer.[26,27] Equal force constants for the partial bonds of A and B to –L are expected at the transition state for thermoneutral proton transfer ($\Delta G^o = 0$, Scheme 6), so that there should be no net movement of -L associated with this symmetrical stretch, and no effect of an –H for –D substitution on this stretching frequency. Hammond-type movement of hydron -L toward the acid catalyst or base acceptor will be observed,[60] respectively, for a change to thermodynamically favorable hydron transfer ($\Delta G^o << 0$, Scheme 6), where the hydron is bonded most tightly to A, or to thermodynamically unfavorable transfer ($\Delta G^o >> 0$) where the hydron is bonded most tightly to B. In both cases, a part of the zero-point energy of the reactant A-L bond is maintained at the symmetrical stretching vibration, which will show a larger frequency for the light isotope –H compared with –D.

There is a Hammond effect on protonation of **X-1** by substituted carboxylic acids. This results in a 0.10 unit increase in the Brønsted parameter α for catalysis by carboxylic acids as the thermodynamic barrier for proton transfer is increased by 9 kcal/mole by changing the substituent at **X-1** from 4-MeO- to 3,5 di-NO_2.[24] This Hammond-type shift in the position of the reaction transition state provides a simple explanation for the decrease in the PIE with the increasing thermodynamic barrier to proton transfer.

(2) It has been proposed that the contribution of tunneling increases with the size of the tunneling *cross section*; and, that this *cross section* is a maximum for thermoneutral hydron transfer, but decreases in size as ΔG^o for proton transfer becomes either positive or negative.[25] This would cause the isotope effect to change from a large tunneling-enhanced value for thermoneutral proton transfer, to the smaller values for more activation limited thermodynamically favorable or unfavorable proton transfer.

The value of $[(E_a)_H - (E_a)_D] = -1.2$ kcal/mole calculated from the slopes of the Arrhenius-type plots shown in Figure 5 is roughly equal to the difference in the zero-point energy of the ground-state LO-L bond. This is consistent with a reaction in which the *zpe* of the hydron is lost at the potential energy maximum for the transition state.. The ratio of $(A_H/A_D) = 1.0$ for the preexponential factors is also consistent with a semiclassical model for proton transfer, where the rate constants for reaction of A–H and A–D approach the same limiting value at very high temperatures. The ratio of $(A_H/A_D) = 1.0$ is inconsistent with a reaction in which there is significant quantum mechanical tunneling of the light, but not the heavy isotope.[61–63] In this case, there should be a sharp increase, with increasing *T*, in the rate of the activation-limited reaction of A–D relative to the rate of the (partly) tunneling-limited reaction of A–H. This would give rise to a sharp decrease in the PIE with increasing *T*, so that extrapolation of the ln

PIE to 1/T = 0 would show a *negative y*-intercept. A unit ratio for the preexponential term is also inconsistent with significant tunneling for the reactions of both –H and –D. The isotope effect on a reaction where both isotopes tunnel through the barrier will show a small or negligible temperature-dependence, so that extrapolation of ln PIE to 1/T = 0 would give a *positive y*-intercept.[61–63] We conclude that protonation of **X-1** by Brønsted acids in water appears to proceed mainly by a mechanism where the reactions of both -H and –D pass over a maximum on the potential energy surface, instead of tunneling through the energy barrier.

Structure-Reactivity Relationships

The primary deuterium isotope effect maximum observed for thermoneutral protonation of **X-1** is consistent with a transition state for proton transfer in which the hydron remains stationary during the symmetrical stretch shown in Scheme 6. [26,27] This corresponds to a transition state in which bond cleavage at the carboxylic acid and bond formation to carbon are each *ca* 50% of that observed for the overall proton transfer reaction (Figure 7).

By comparison, the structure reactivity parameters $\alpha = 0.66$ and $\beta = 0.58$ (Scheme 7)[24] estimated for thermoneutral protonation of **X-1** by substituted carboxylic acids are significantly greater than the values of $\alpha = \beta = 0.50$ predicted by simple Marcus theory. [6,65] These Brønsted parameters are consistent with the development of an effective transition state charge of −0.66 at the carboxylic acid catalyst and of +0.58 at the carbon acid base,[66,67] where the charges are normalized relative to values of -1 for the ionization substituted carboxylic acid and of +1 for protonation of **X-1** to form the oxocarbenium ion **X-2**$^+$.

We propose that there is a balanced transition state for proton transfer, as suggested by the position of the isotope effect maximum, and that the Brønsted structure-reactivity parameter α (Scheme 7) overestimates the fractional proton transfer from the acid catalyst. This would be the case if the total change in *effective* charge on proceeding from free reactants to the ion pair product complex is greater than the change of −1.0 assumed for ionization of carboxylic acids in water,[64] and if solvation of the developing carboxylate anion (K_{sol}, Figure 7) lags behind proton transfer to the carbon base.[4,5,68] This is shown in Figure 7, where formation of hydrogen bonds between solvent and the carboxylate anion reduces the charge at the oxygen anion, so that K_{sol} for anion solvation increases with increasing pK_a of the carboxylic acid catalyst. A value of $\alpha_{sol} = -0.20$ has been estimated for conversion of complexes between substituted quinuclidines and activated phosphate monoesters (*e.g.* 2,4-dinitrophenyl phosphate) to the free solvated quinuclidine.[64] A similar value of $\alpha_{sol} = -0.20$ for formation of hydrogen bonds to the carboxylate anion would give a total absolute *effective* charge of $(1 - \alpha_{sol}) = 1.20$ at RCO_2^- in the ion-pair complex (Figure 7).[65] In this case, the *effective* change in charge at the carboxyl(ate) oxygen on moving from reactant to transition state ($\alpha = 0.66$, Scheme 7) would be only slightly greater than 50% of the total charge of 1.2 at the product complex: $\alpha_{nor} = \alpha_{obs}/(1 - \alpha_{sol}) = 0.66/1.20 = 0.55$. This is closer to the value of 0.50 predicted by Marcus theory for a thermoneutral proton transfer reaction.

Computational studies

We have compared these experimentally determined isotope effects with isotope effects calculated using a novel approach based on Kleinert's variational perturbation theory within the framework of Feynman path integrals.[20–22] There is generally good agreement between the results of experiments and calculations, and the computational results provide additional deeper insight into origin of these primary isotope effects.

Supplementary Material

Refer to Web version on PubMed Central for supplementary material.

Acknowledgments

This paper is dedicated to Yvonne Chiang and A. Jerry Kresge. We acknowledge the National Institutes of Health (GM 39754) for generous support of this work.

REFFERENCES

1. Hynes, JT.; Klinman, JP.; Limbach, H-H.; Schowen, RL. Hyrogen Transfer Reactions. Weinheim: Wiley-VCH; 2007.
2. Jencks WP. Bull. Soc. Chim. France 1988:218–224.
3. Jencks WP. Chem. Rev 1985;85:511–527.
4. Bernasconi CF. Acc. Chem. Res 1992;25:9–16.
5. Bernasconi CF. Acc. Chem. Res 1987;20:301–308.
6. Kresge AJ. Chem. Soc. Rev 1973;2:475–503.
7. Bernasconi CF, Wenzel PJ. J. Am. Chem. Soc 1994;116:5405–5413.
8. Bernasconi CF, Wenzel PJ. J. Org. Chem 2003;68:6870–6879. [PubMed: 12946125]
9. Sato M, Kitamura Y, Yoshimura N, Yamataka H. J. Org. Chem 2009;74:1268–1274. [PubMed: 19123838]
10. Kiefer PM, Hynes JT. J. Phys. Chem. A 2004;108:11809–11818.
11. Costentin C, Saveant J-M. J. Am. Chem. Soc 2004;126:14787–14795. [PubMed: 15535704]
12. Saunders WH. J. Am. Chem. Soc 1994;116:5400–5404.
13. Heeb LR, Peters KS. J. Phys. Chem. B 2008;112:219–226. [PubMed: 17929858]
14. Fillaux F, Cousson A, Gutmann MJ. Pure. App. Chem 2007;79:1023–1039.
15. Cui Q, Karplus M. J. Am. Chem. Soc 2002;124:3093–3124. [PubMed: 11902900]
16. Gao J, Wong K-Y, Major DT. J. Comp. Chem 2007;29:514–522. [PubMed: 17722009]
17. Truhlar DG, Gao J, Alhambra C, Garcia-Viloca M, Corchado J, Sanchez ML, Villa J. Acc. Chem. Res 2002;35:341–349. [PubMed: 12069618]
18. Alhambra C, Gao J, Corchado JC, Villa J, Truhlar DG. J. Am. Chem. Soc 1999;121:2253–2258.
19. Tsang W-Y, Richard JP. J. Am. Chem. Soc 2007;129:10330–10331. [PubMed: 17676848]
20. Wong K-Y, Richard JP, Gao J. J. Am. Chem. Soc. 2009 Following paper in this issue.
21. Wong K-Y, Gao J. J. Chem. Theory Comput 2008;4:1409–1422. [PubMed: 19749977]
22. Wong K-Y, Gao J. J. Chem. Phys 2007;127:211103. [PubMed: 18067342]
23. Kresge AJ, Sagatys DS, Chen HL. J. Am. Chem. Soc 1977;99:7228–7233.
24. Richard JP, Williams KB. J. Am. Chem. Soc 2007;129:6952–6961. [PubMed: 17488079]
25. Bell, RP. The Proton in Chemistry. Second ed.. Ithaca, NY: Cornell University Press; 1973. p. 250-296.
26. Westheimer FH. Chem. Rev 1961;61:265–273.
27. Melander, L. Isotope Effects on Reaction Rates. New York: Ronald Press; 1960. p. 24-32.
28. Amyes TL, Richard JP. J. Am. Chem. Soc 1992;114:10297–10302.
29. Amyes TL, Richard JP. J. Am. Chem. Soc 1996;118:3129–3141.
30. Williams, K. Chemistry. Buffalo: University at Buffalo; 1998. p. 208Vol. Ph.D.
31. Richard JP, Nagorski RW. J. Am. Chem. Soc 1999;121:4763–4770.
32. Rios A, Amyes TL, Richard JP. J. Am. Chem. Soc 2000;122:9373–9385.
33. Rios A, Crugeiras J, Amyes TL, Richard JP. J. Am. Chem. Soc 2001;123:7949–7950. [PubMed: 11493086]
34. Richard JP, Williams G, O'Donoghue AC, Amyes TL. J. Am. Chem. Soc 2002;124:2957–2968. [PubMed: 11902887]
35. Rios A, Richard JP, Amyes TL. J. Am. Chem. Soc 2002;124:8251–8259. [PubMed: 12105903]
36. Crugeiras J, Rios A, Amyes TL, Richard JP. Org. Biomol. Chem 2005;3:2145–2149. [PubMed: 15917903]

37. Crugeiras J, Rios A, Riveiros E, Amyes TL, Richard JP. J. Am. Chem. Soc 2008;130:2041–2050. [PubMed: 18198876]
38. Nagorski RW, Richard JP. J. Am. Chem. Soc 2001;123:794–802. [PubMed: 11456612]
39. Rios A, Richard JP. J. Am. Chem. Soc 1997;119:8375–8376.
40. Tanaka N, Thornton ER. J. Am. Chem. Soc 1976;98:1617–1619.
41. Thibblin A. Chem. Soc. Rev 1989;18:209–224.
42. Hegarty A, Dowling J, Eustace S, McGarraghy M. J. Am. Chem. Soc 1998;120:2290–2296.
43. Kresge AJ, Allred AL. J. Am. Chem. Soc 1963;85:1541–1541.
44. Gold V. Proc. Chem. Soc. Lon 1963:141–143.
45. Jarret RM, Saunders M. J. Am. Chem. Soc 1986;108:7549–7553.
46. Kresge AJ, Chen H-L, Chiang Y, Murrill E, Payne MA, Sagatys DS. J. Am. Chem. Soc 1971;93:413–423.
47. Loudon GM, Smith CK, Zimmerman SE. J. Am. Chem. Soc 1974;96
48. Richard JP, Williams KB, Amyes TL. J. Am. Chem. Soc 1999;121:8403–8404.
49. Young PR, Jencks WP. J. Am. Chem. Soc 1977;99:8238–8248.
50. Singleton DA, Thomas AA. J. Am. Chem. Soc 1995;117:9357–9358.
51. Jencks, WP. Catalysis in Chemistry and Enzymology. New York: Dover Publications; 1987. p. 268-272.
52. Kresge, AJ.; O'Ferrall, RAM.; Powell, MF. Isotopes in Organic Chemistry. Buncel, E., editor. Amsterdam: Elsevier; 1987. p. 178-275.
53. Schowen RL. Prog. Phys. Org. Chem 1972;9:275–332.
54. Kreevoy MM, Steinwand PJ, Kayser WV. J. Am. Chem. Soc 1966;88:124–131.
55. Lowrey, TH.; Richardson, KS. Mechanism and Theory in Organic Chemistry. New York: Harper & Row; 1987. p. 233-236.
56. O'Ferrall RAM, Koeppl GW, Kresge AJ. J. Am. Chem. Soc 1971;93:1–9.
57. Bell, RP. The Proton in Chemistry. Second ed.. Ithaca, NY: Cornell University Press; 1973. p. 265
58. Bigeleisen J, Mayer MG. J. Chem. Phys 1947;15
59. Bigeleisen J, Wolfsberg M. Adv. Chem. Phys 1958;1:15–76.
60. Hammond GS. J. Am. Chem. Soc 1955;77:334–338.
61. Kohen, A. Isotope Effects in Chemistry and Biology. Kohen, A.; Limbach, H-H., editors. New York: Taylor & Francis; 2006. p. 743-764.
62. Kohen A, Klinman JP. Acc. Chem. Res 1998;31:397–404.
63. Kwart H. Acc. Chem. Res 1982;15:401–408.
64. Jencks WP, Haber MT, Herschlag D, Nazaretian KL. J. Am. Chem. Soc 1986;108:479–483.
65. Marcus RA. J. Phys. Chem 1968;72:891–899.
66. Hupe DJ, Jencks WP. J. Am. Chem. Soc 1977;99:451–464.
67. Williams A. Adv. Phys. Org. Chem 1992;27:1–55.
68. Bernasconi CF, Wiersema D, Stronach MW. J. Org. Chem 1993;58:217–223.

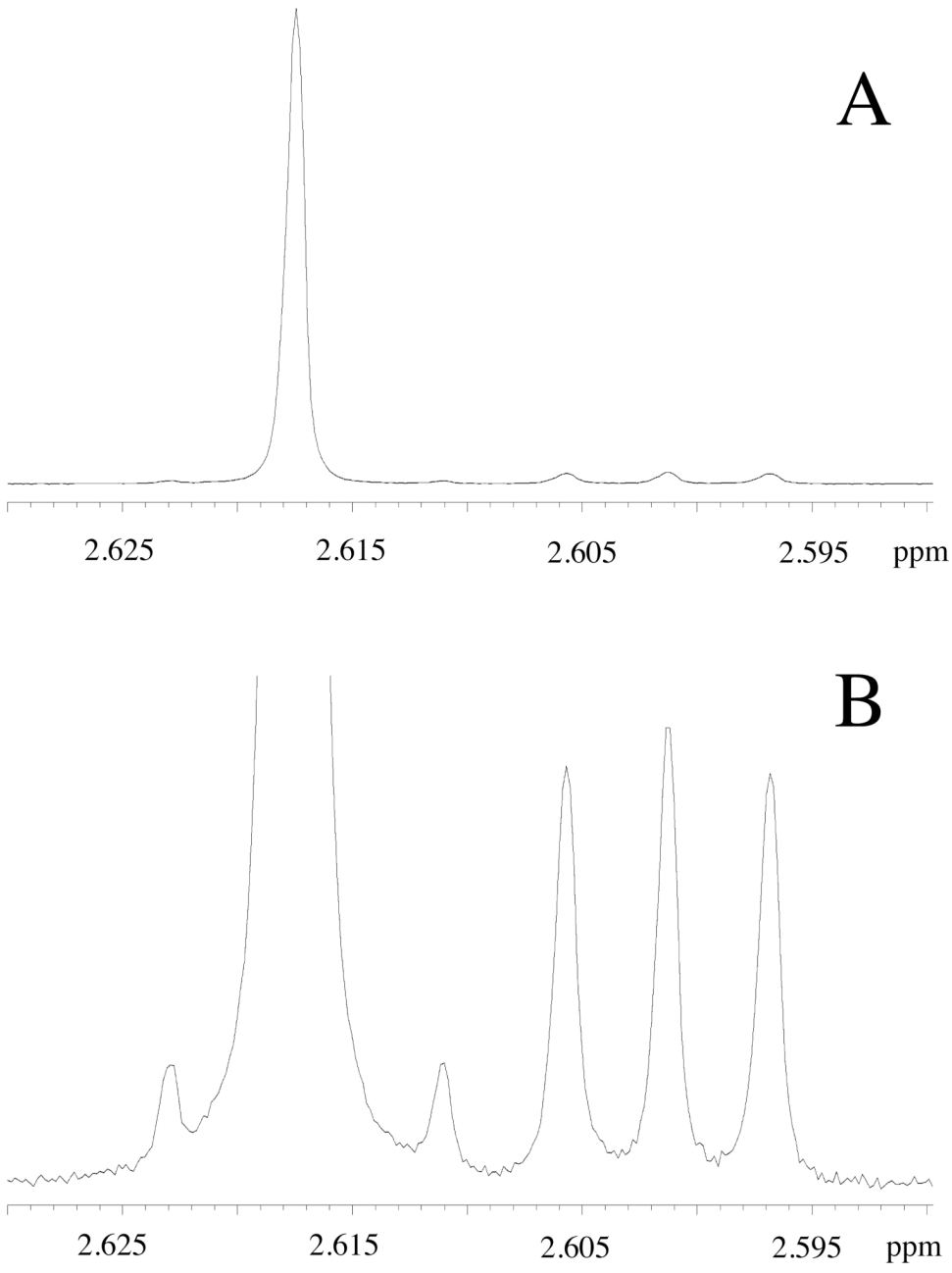

Figure 1.
Partial ^{1}H NMR spectrum (recorded in $CDCl_3$) at 500 MHz of **H-3** formed by lyonium ion-catalyzed hydrolysis of **H-1** in 50/50 (v/v) HOH/DOD (*I* = 1.0, KCl) at 25 °C. The same spectrum is shown at two different resolutions. The small peaks on either side of the singlet at 2.614 ppm are ^{13}C satellites from coupling of the α–CH_3 protons to the neighboring carbonyl carbon.[28] The peak assignments are given in the text.

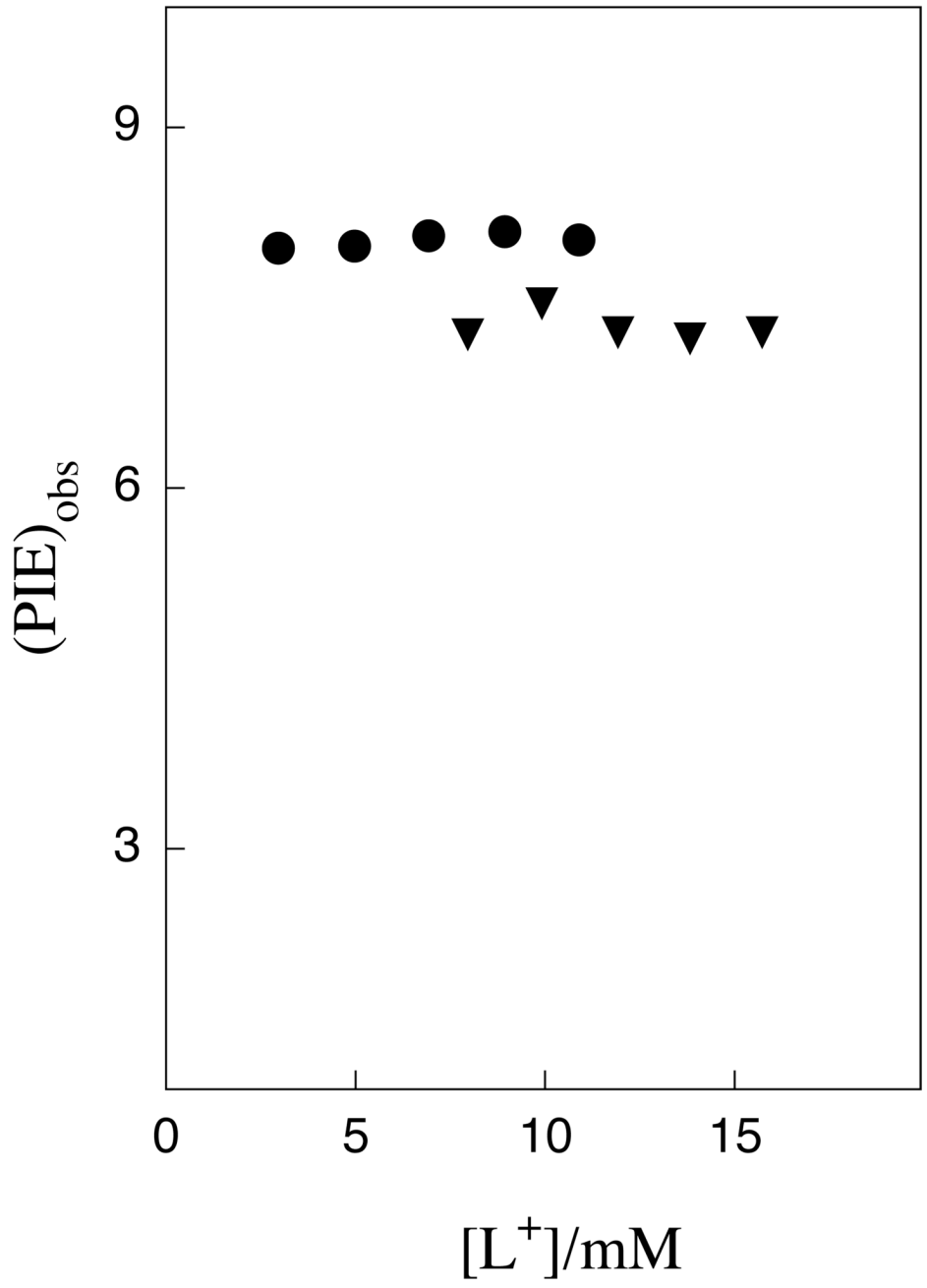

Figure 2.
Product deuterium isotope effects for lyonium ion-catalyzed protonation of **X-1** in 50/50 (v/v) HOH/DOD (*I* = 1.0, KCl). Key: (●), **4-MeO-1**; (▼), **3,5-di-NO_2-1**.

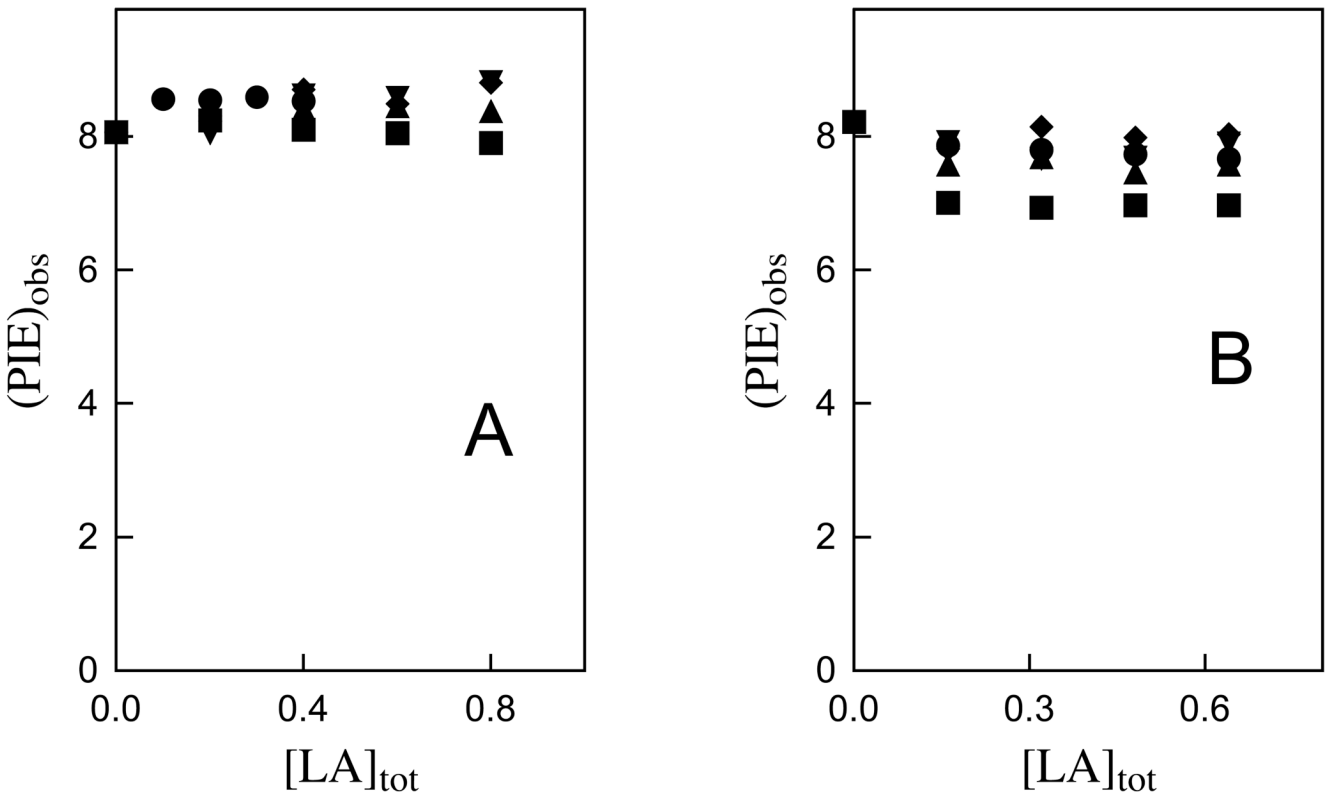

Figure 3.

The effect of increasing [RCO_2H] on the observed PIE for the reactions of **X-1** in 50/50 (v/v) HOH/DOD at 25 °C and *I* = 1.0 (KCl). (A) Data for **4-MeO-1**. Key: (■), acetic acid buffer ([AH]/[A−] = 1/9; (▲), methoxyacetic acid buffer ([AH]/[A^-] = 1/9; (●), chloroacetic acid buffer ([AH]/[A^-] = 1/9; (◆), cyanoacetic acid buffer ([AH]/[A^-] = 1/9; (▼), dichloroacetic acid buffer ([AH]/[A−] = 1/9. (B) Data for **4-H-1**. Key: (■), acetic acid buffer ([AH]/[A^-] = 1.0; (▲), methoxyacetic acid buffer ([AH]/[A^-] = 1/9; (●), chloroacetic acid buffer ([AH]/[A^-] = 1/9; (◆), cyanoacetic acid buffer ([AH]/[A^-] = 1/9; (▼), dichloroacetic acid buffer ([AH]/[A^-] = 1/9.

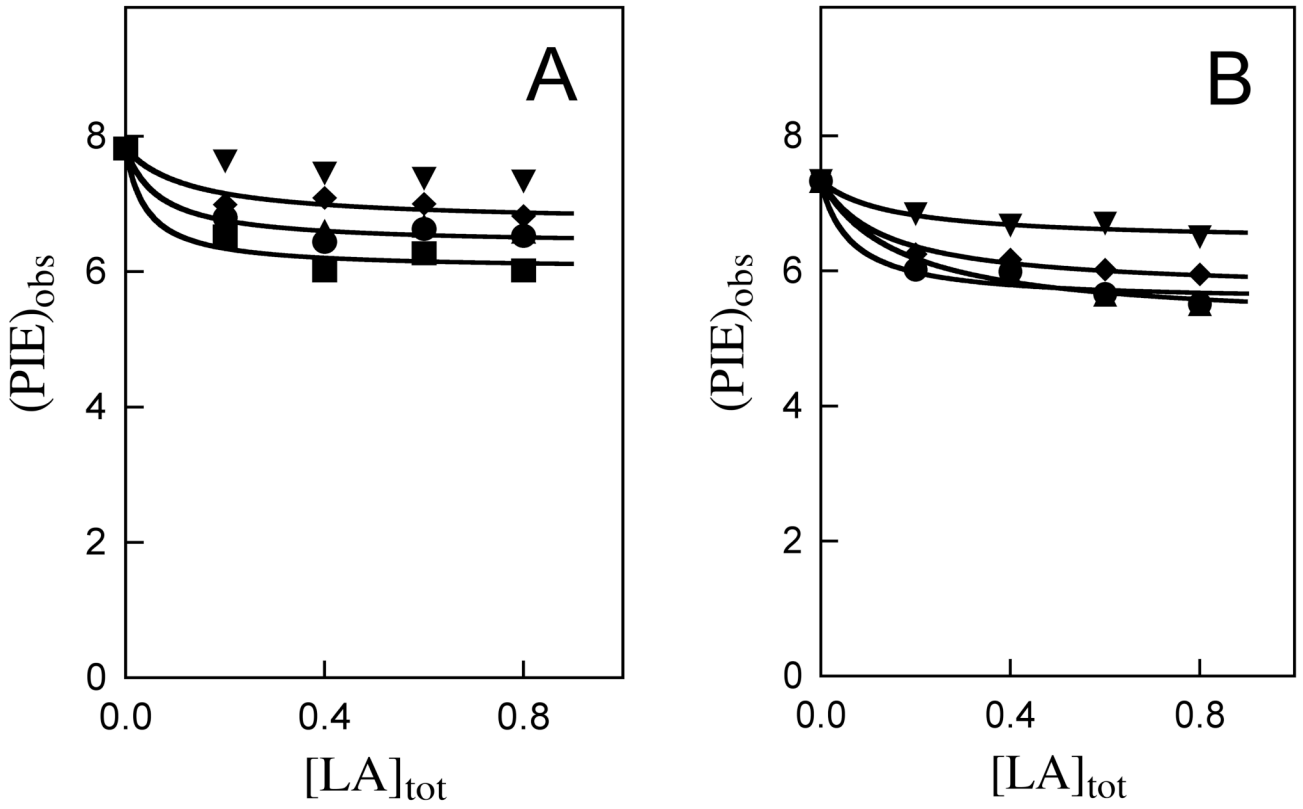

Figure 4.

The effect of increasing [RCO_2H] on the PIE for the reactions of **X-1** in 50/50 (v/v) HOH/DOD at 25 °C and *I* = 1.0 (KCl). (A) Data for **4-NO_2-1**. Key: (■), acetic acid buffer ([AH]/[A^-] = 1.0; (▲), methoxyacetic acid buffer ([AH]/[A^-] = 1/9; (●), chloroacetic acid buffer ([AH]/[A^-] = 1/9; (◆), cyanoacetic acid buffer ([AH]/[A^-] = 1/9; (▼), dichloroacetic acid buffer ([AH]/[A^-] = 1/9. The lines showing the fit of data for the chloroacetic- and methoxyacetic acid-catalyzed reactions are nearly superimposible. (B) Data for **3,5-di-NO_2-1**. Key: (▲), methoxyacetic acid buffer ([AH]/[A^-] = 7/3; (●),chloroacetic acid buffer ([AH]/[A^-] = 1/9; (◆),cyanoacetic acid buffer ([AH]/[A^-] = 1/9; (▼), dichloroacetic buffer ([AH]/[A^-] = 1/9.

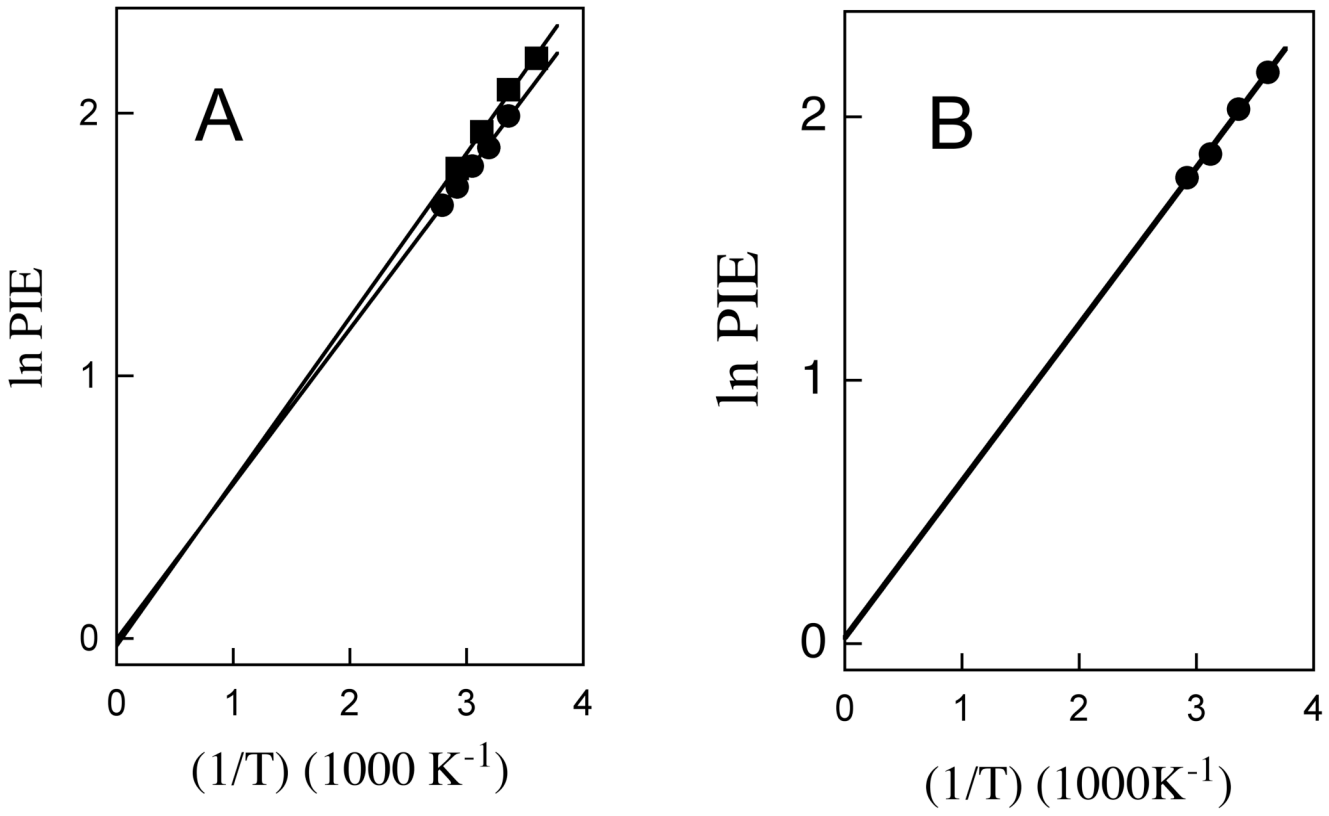

Figure 5.
(A) Arrhenius-type plots of $(PIE)_L$ for the protonation of **4-MeO-1** (■) and **3,5-di-NO_2-1** (●) by lyonium ion in 50/50 HOH/DOD at I = 1.0 (KCl). (B) Arrhenius-type plot of $(PIE)_{AL}$ for protonation of **H-1** by methoxyacetic acid in 50/50 HOH/DOD at I = 1.0 (KCl).

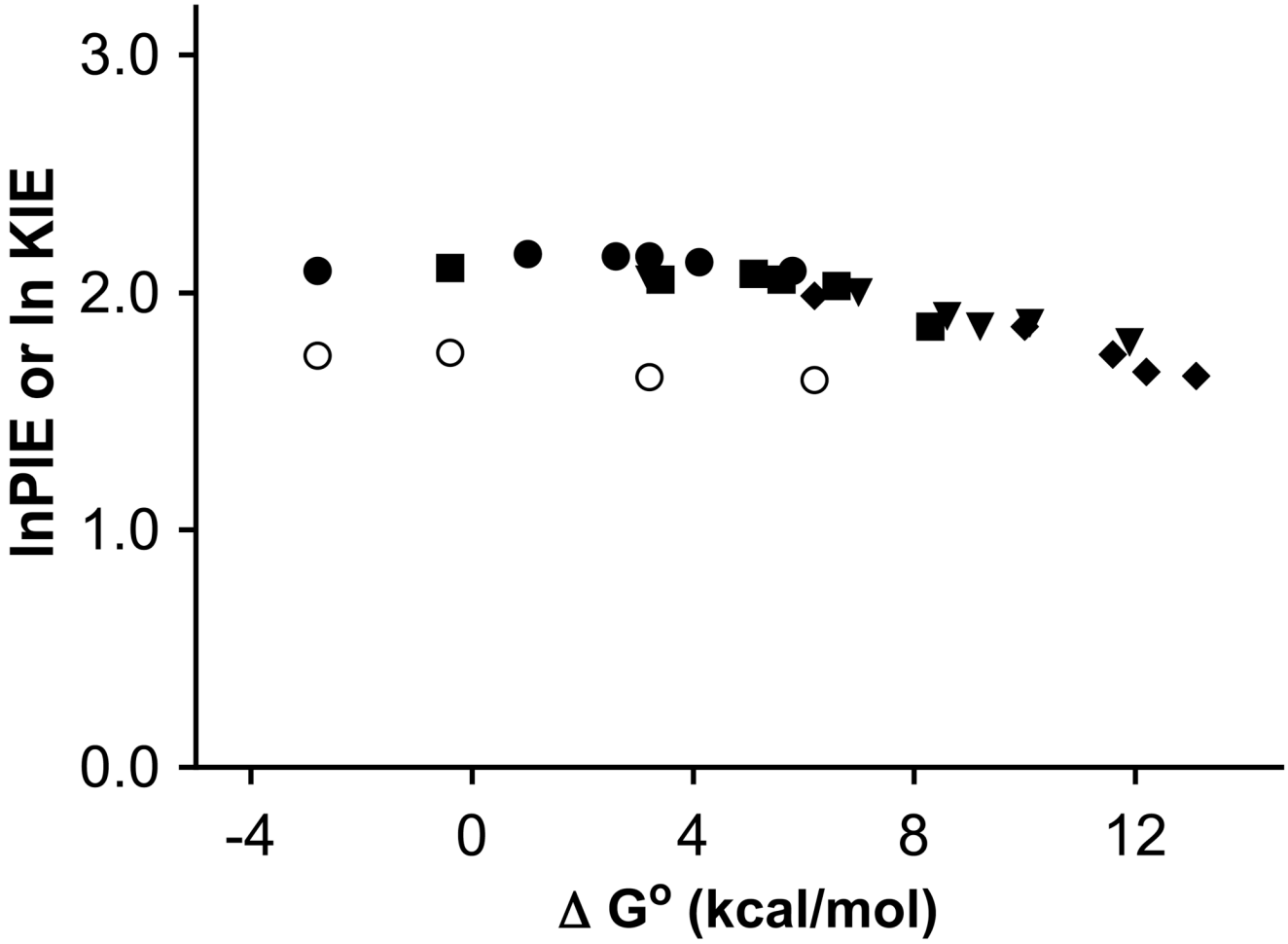

Figure 6.

The effect of changing thermodynamic driving force on the product isotope effects (PIE) and the kinetic isotope effects (KIE) for protonation of **X-1** in 50/50 HOH/DOD at I = 1.0 (KCl) to form the corresponding oxocarbenium ion **X-2**$^{+}$. The solid symbols show PIEs. Key: (●), protonation of **4-MeO-1**; (■), protonation of **H-1**; (▼), protonation of **4-NO$_2$-1**; (◆), protonation of **3,5-di-NO$_2$-1**. The open symbols show the values of the KIE for protonation of **X-1** by lyonium ion.

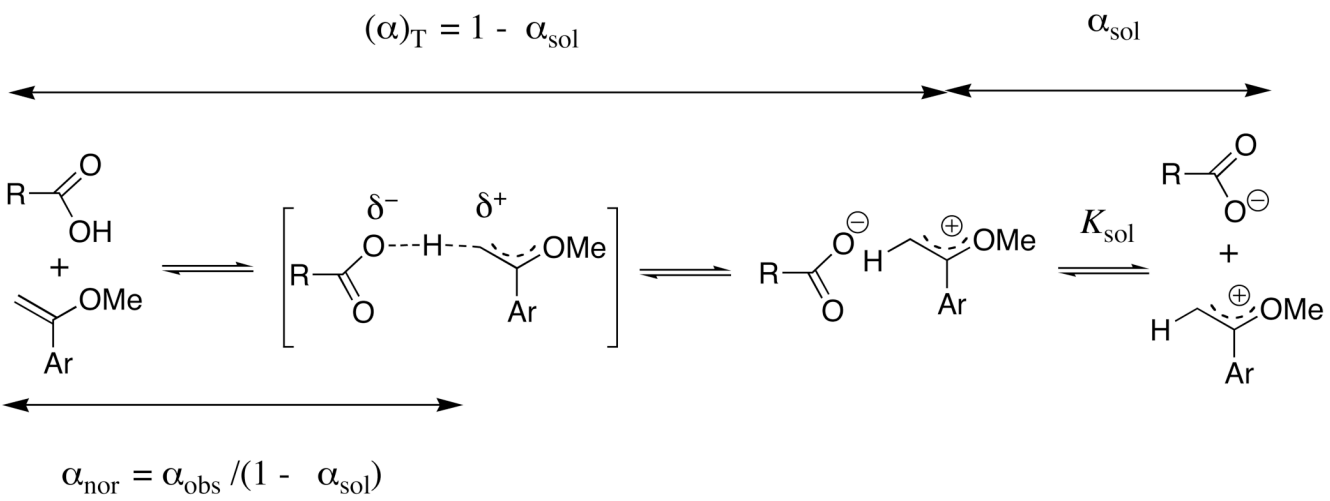

Figure 7.

A reaction where proton transfer from the carboxylic acid to the carbon base to form an ion pair, is followed by full solvation of the anion with a value of $\alpha_{solv} = -0.20$.[64] The effective negative charge at the product complex ($1 - \alpha_{solv} = 1.2$) is used to obtain a normalized Brønsted parameter α_{nor}; $\alpha_{nor} = \alpha_{obs}/(1 - \alpha_{sol})$ which provides a more realistic measure of the position of the transition state relative to the ion-pair product complex.

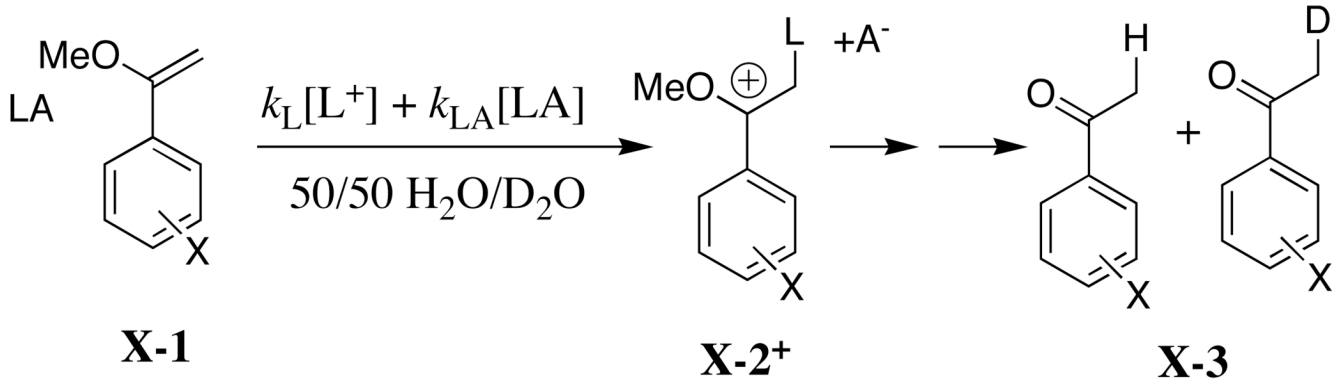

Scheme 1.

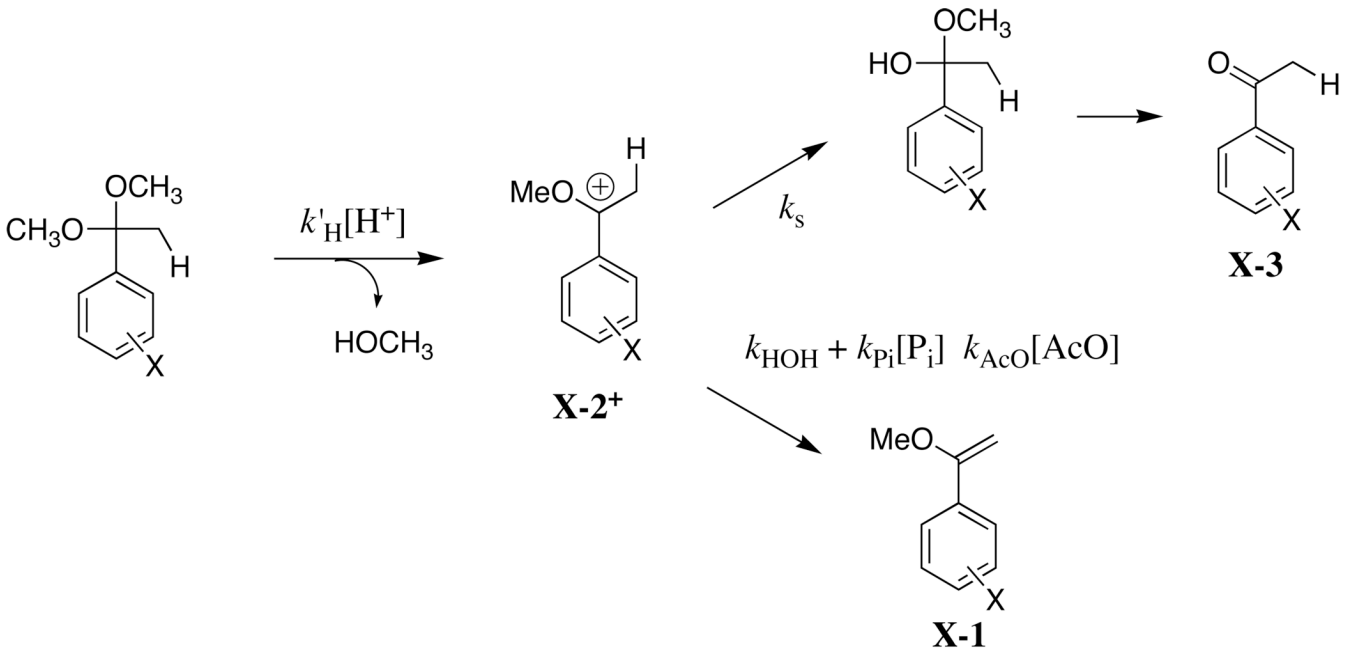

Scheme 2.

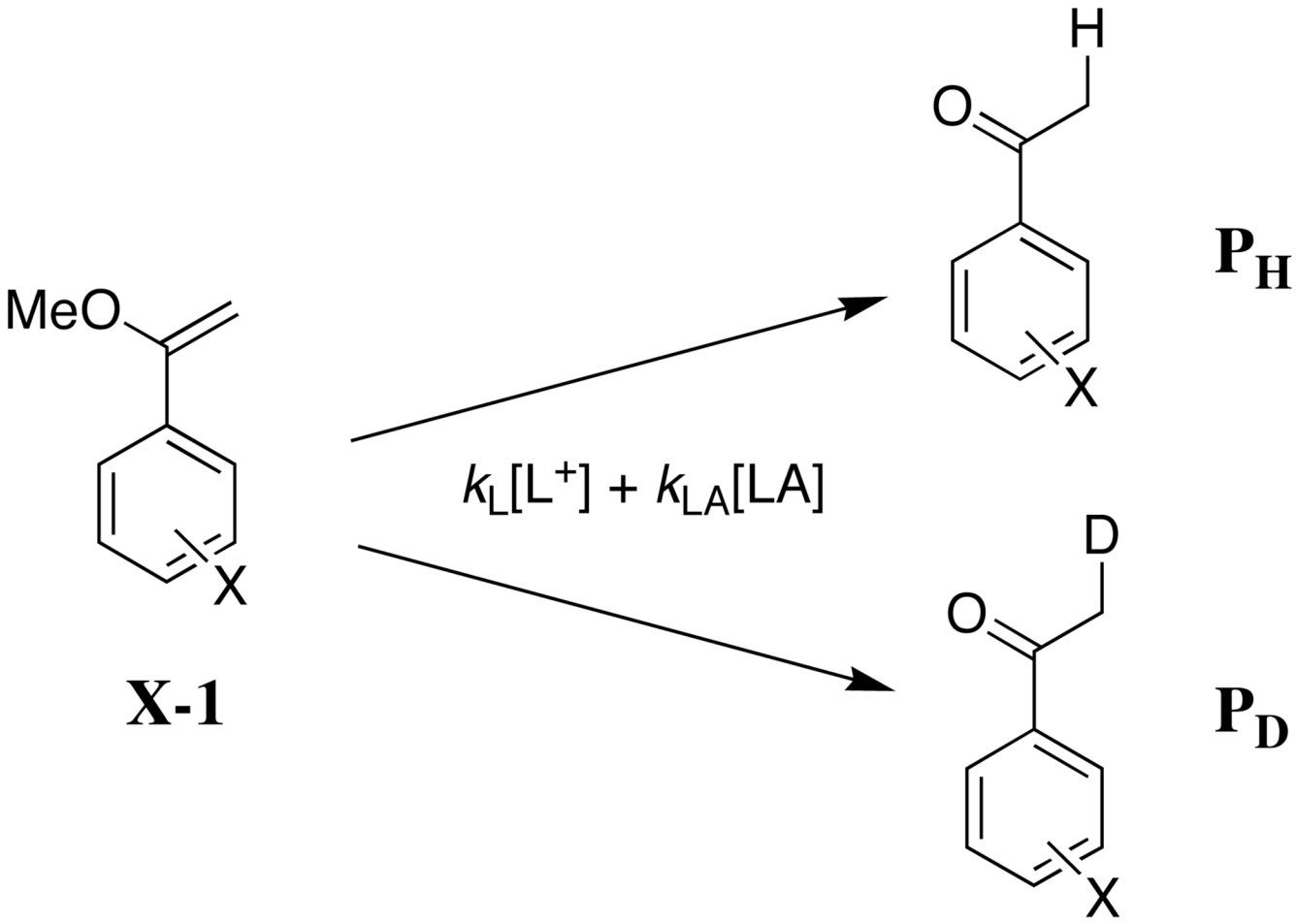

Scheme 3.

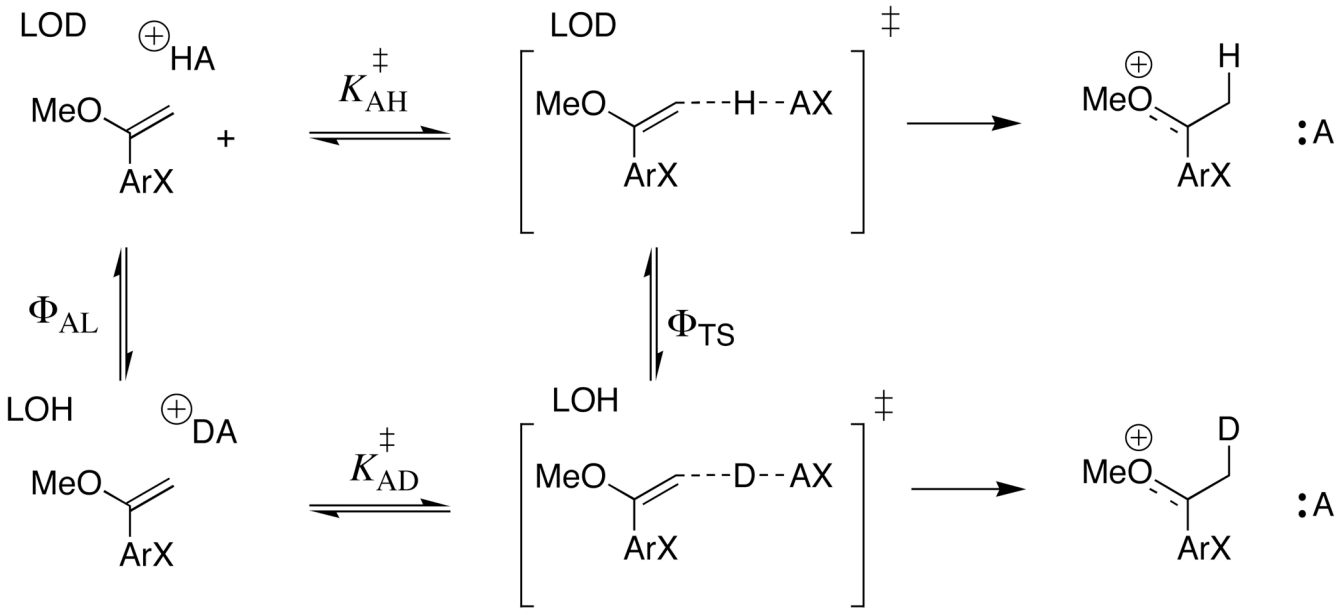

Scheme 4.

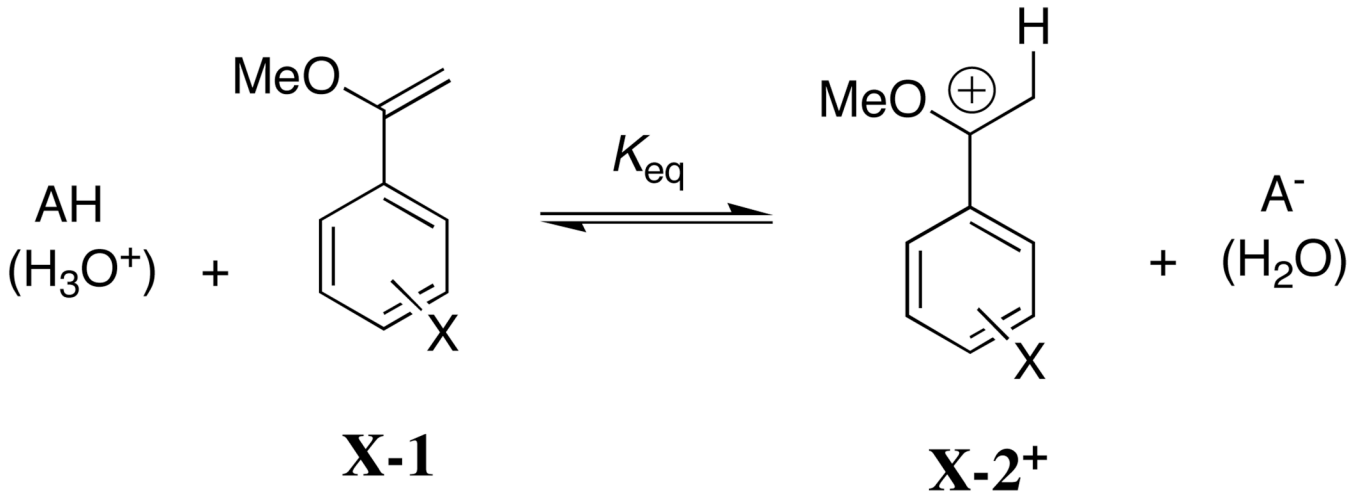

X-1 **X-2+**

Scheme 5.

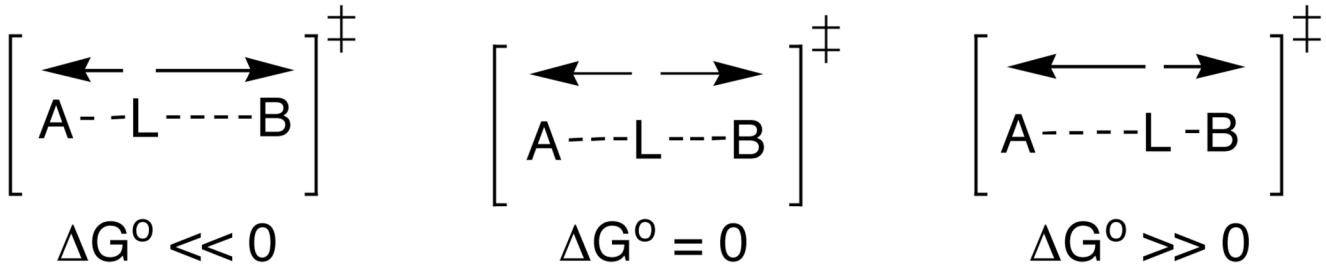

Scheme 6.

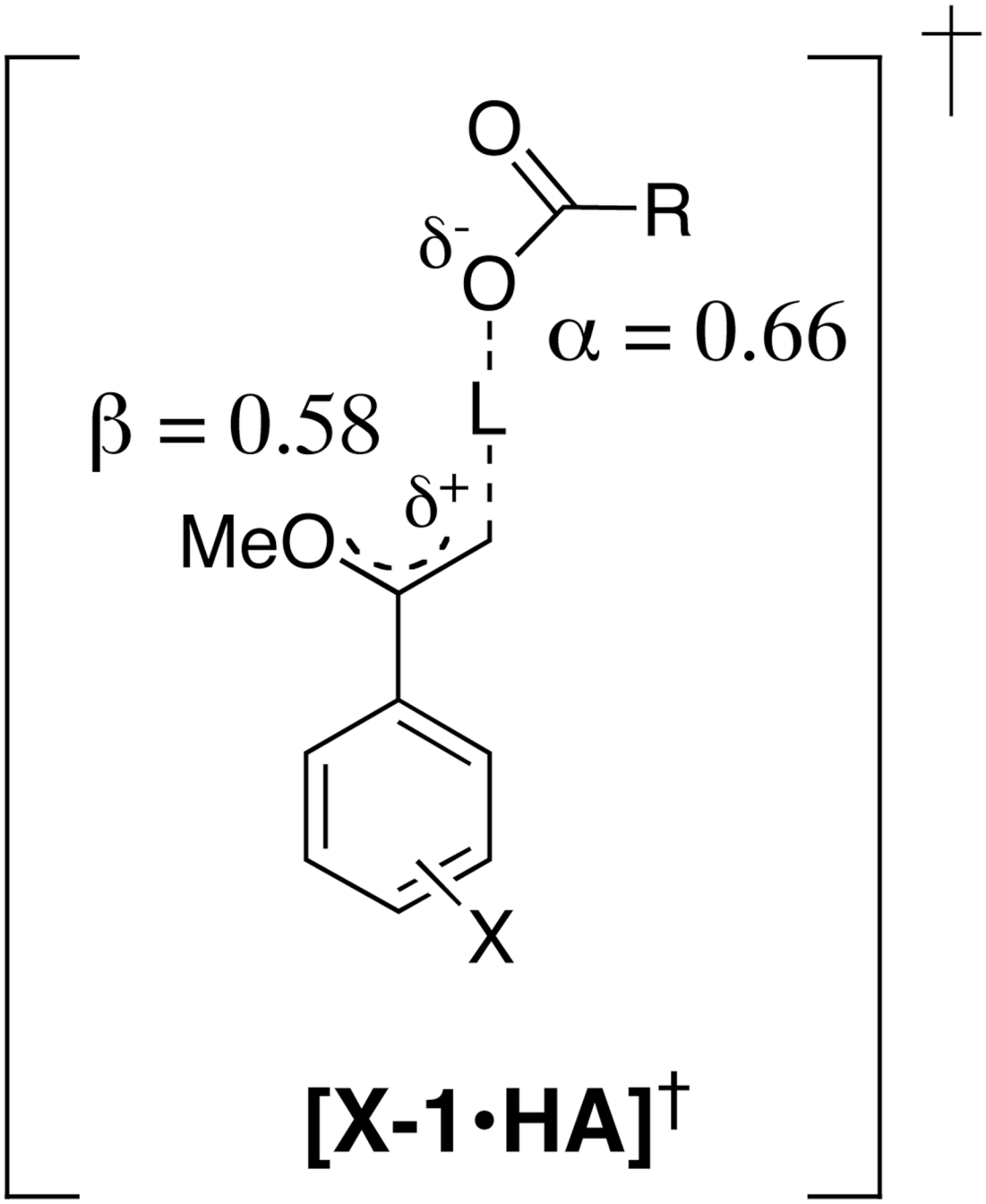

Scheme 7.

Table 1

Product Isotope Effects and Derived Kinetic Isotope Effects on Hydron Transfer from L_3O^+ and Substituted Carboxylic Acids to **X-1** in 50/50 (v/v) HOH/DOD at 25°C and I = 1.0 (KCl).

			Product Isotope Effect			
	$pK_a^{H_2O}$,[a]		**4-OMe** [b]	**-H** [b]	**4-NO_2** [c]	**3,5-di-NO_2** [c]
L^+	−1.76	PIE [b]	8.1 ± 0.1	8.2 ± 0.2	7.8 ± 0.1	7.3 ± 0.2
		KIE [e]	5.6	5.7	5.4	5.0
$Cl_2CHCOOL$	1.03	PIE	8.7 ±0.2	7.7 ± 0.1	7.4 ± 0.2 [d]	6.4 ± 0.1
CNCHCOOL	2.23	PIE	8.7 ± 0.3	8.0 ± 0.2	6.7 ± 0.1	5.7 ± 0.1
$ClCH_2COOL$	2.65	PIE	8.6 ± 0.1	7.7 ± 0.1	6.4 ± 0.1	5.3 ± 0.1
$MeOCH_2COOL$	3.33	PIE	8.4 ± 0.1	7.6 ± 0.1	6.5 ± 0.1	5.1 ± 0.1
CH_3COOL	4.60	PIE	8.1 ± 0.2	7.0 ± 0.1	6.0 ± 0.1	
		KIE [f]	7.3	6.3	5.4	

[a] pK_as determined in H_2O: Fox, J. P.; Jencks, W. P. *J. Am. Chem. Soc.* **1974**, *96*, 1436–1449.

[b] Calculated as the average of the values of $(PIE)_{obs}$ determined at several different concentrations of the catalyzing acid.

[c] Unless noted otherwise, the values of $(PIE)_{AL}$ for the carboxylic acid-catalyzed reactions were obtained from a nonlinear least squares fit of the data in Figures 4A and 4B to eq 8 (see text).

[d] Calculated as the average of the values of $(PIE)_{obs}$ determined for reactions at 0.40, 0.60 and 0.80 M buffer.

[e] $KIE = \Phi_L(PIE)_L$, where $\Phi_L = 0.69$.[43,44]

[f] $KIE = \Phi_{AL}(PIE)_{AL}$, where $\Phi_{AL} = 0.9$.[45]

Table 2

Second-Order Rate Constants for Acid-Catalyzed Hydrolysis of **X-1** and for the Base-Catalyzed Exchange of the First α-CH_3 Hydrogen of **X-3** for Deuterium from Solvent.[a]

Acid	k_{LA} (M^{-1} s^{-1}) [b]		k_A (M^{-1} s^{-1}) [c]	
	4-NO_2	**3,5-di-NO_2**	**4-NO_2**	**3,5-di-NO_2**
L^+	1.1	7.1×10^{-2}		
$Cl_2CHCOOL$		2.0×10^{-2}		
CNCHCOOL	2.3×10^{-2}	1.4×10^{-3}		
$ClCH_2COOL$	1.7×10^{-2}	9.45×10^{-4}		
$MeOCH_2COOL$	4.6×10^{-3}	2.8×10^{-4}	3.7×10^{-7} [d]	1.2×10^{-6} [d]
CH_3COOL	6.7×10^{-4}	2.4×10^{-5} [f]	1.5×10^{-6} [g]	

[a] For reactions in 50/50 (v/v) HOH/DOD at 25 °C and I = 1.0 (KCl).

[b] Second-order rate constants for Brønsted acid-catalyzed hydrolysis of **X-1** in 50/50 (v/v) HOH/DOD determined as the slope of a plot of 4 – 5 values of k_{obs} against the concentration of the buffer acid catalyst, unless noted otherwise

[c] Second-order rate constant for Brønsted base-catalyzed deprotonation of **X-3** in 50/50 (v/v) HOH/DOD determined by monitoring incorporation of deuterium into the α-CH_3 group of the ketone by ^1H NMR.

[d] Estimated from $k_{obs} = 2.6 \times 10^{-7}$ s^{-1} for the reaction catalyzed by 0.80 M methoxyacetic acid buffer ($[A^-]/[AH] = 9$).

[e] Estimated from $k_{obs} = 8.8 \times 10^{-6}$ s^{-1} for the reaction catalyzed by 0.80 M methoxyacetic acid buffer ($[A^-]/[AH] = 9$).

[f] Calculated assuming $k_{AcO}/k_{MeOAc} = 11$ for protonation of **3,5-di-NO_2** by acetic and methoxyacetic acid is the same for reactions in HOH [24] and in 50/50 (v/v) HOH/DOD

[g] Calculated from $k_{obs} = 1.1 \times 10^{-6}$ $s^{-1} = k_A/[A^-]$ for the reaction catalyzed by 0.80 M acetic acid buffer ($[A^-]/[AH] = 9$).

Table 3

Product Isotope Effects on Proton Transfer from Lyonium Ion and Methoxyacetic Acid to Ring-Substituted α-Methoxystyrenes in 50/50 (v/v) HOH/DOD at I = 1.0 (KCl) Determined for Reactions at Several Different Temperatures.

X-1	T (K)	Acid	$(PIE)_L$ [a]
MeO-1	278	L_3O^+	9.1 ± 0.2 [b]
	320	L_3O^+	6.9 ± 0.1 [c]
	343	L_3O^+	5.9 ± 0.1 [c]
3,5-di-NO_2-1	313	L_3O^+	6.5 ± 0.2 [b]
	328	L_3O^+	6.0 ± 0.1 [b]
	343	L_3O^+	5.6 ± 0.1 [b]
	359	L_3O^+	5.2 ± 0.1 [b]
			$(PIE)_{AL}$ [d]
H-1	277	$MeOCH_2COOL$	8.8 ± 0.3
	321	$MeOCH_2COOL$	6.4 ± 0.2
	343	$MeOCH_2COOL$	5.9 ± 0.1

[a] The PIE on lyonium ion-catalyzed protonation of **X-1** (eq 5).

[b] The average of the values of $(PIE)_{obs}$ (eq 2) determined for reactions at several different $[L_3O^+]$.

[c] Determined as described in text.

[d] The product isotope effect on methoxyacetic acid-catalyzed protonation of **X-1** (eq 6), calculated as the average four buffer independent values of $(PIE)_{obs}$.